SCIENCE CHINA
Information Sciences

• REVIEW •

April 2019, Vol. 62 041301:1–041301:32
https://doi.org/10.1007/s11432-018-9742-0

Development status of high power fiber lasers and their coherent beam combination†

Zejin LIU, Xiaoxi JIN, Rongtao SU, Pengfei MA & Pu ZHOU

College of Advanced Interdisciplinary Studies, National University of Defense Technology, Changsha 410073*, China*

Received 11 May 2018/Revised 13 November 2018/Accepted 7 December 2018/Published online 27 February 2019

Abstract High-power fiber laser has been emerged great potential in a wide range of applications and becomes a robust candidate for high energy solid state laser system. To further increase the output brightness of single-channel fiber laser, high-brightness pump sources and high-power-handling passive components should be fabricated and utilized in the fiber laser systems, in addition to the advanced techniques for multiple nonlinear effects managements. The state-of-the-art high power fiber lasers are reviewed, in terms of narrow-linewidth fiber lasers, broadband fiber lasers and fiber lasers at 2 μm. Coherent beam combining is a promising technique to obtain higher output power while maintaining excellent beam quality simultaneously, which breaks through the bottlenecks of single-channel fiber laser. Based on a series of key techniques for coherent beam combining, high-power coherent beam combining of fiber lasers could be enabled with high combining efficiency. In this paper, we review the progress of high-power fiber lasers and their coherent beam combining in the recent decade, particularly the relevant work in our group. The future prospects of fiber lasers and coherent beam combining technique are also discussed.

Keywords fiber lasers and amplifiers, nonlinear effects and mode instability, coherent beam combining, passive components, 2 μm fiber lasers

Citation Liu Z J, Jin X X, Su R T, et al. Development status of high power fiber lasers and their coherent beam combination. Sci China Inf Sci, 2019, 62(4): 041301, https://doi.org/10.1007/s11432-018-9742-0

1 Introduction

Fiber laser was one of the first several kinds of lasers demonstrated since the invention of laser [1]. Historically, fiber laser has been treated as a low-power high-performance device that had been used in the case such as sensing and telecommunication [2–5], which may be attributed to the relatively late development of brightness-scaling of pump source (typical laser diode) and the core-pumping configuration. Since the late 1980s, with the parallel and rapid development of laser diode and double-cladding fiber that enables cladding-pumping configuration, the output power of fiber laser has been achieved unprecedented increasing speed [6], which has opened a new avenue for application such as high power laser material processing [6, 7]. The optical fiber acts as lasing gain medium and simultaneously a waveguide that confining the laser mode, which could help to significantly increase the beam quality when the laser operates at rather high power level (more than multi-kW level), and the thermal load is also much weakened because of the distribution over a relatively long fiber length [3]. The aforementioned unique properties make fiber laser a hot topic for both academic and industrial communities [8–10]. Nevertheless, it is to be noted that there are several physical limitations for single monolithic fiber laser [11–15], which causes the ∼20 kW level upper-limit output power of a diffraction-limited fiber laser. Beam combining of multiple

* Corresponding author (email: zejinliu@nudt.edu.cn, shandapengfei@126.com, zhoupu203@163.com)
† Invited article

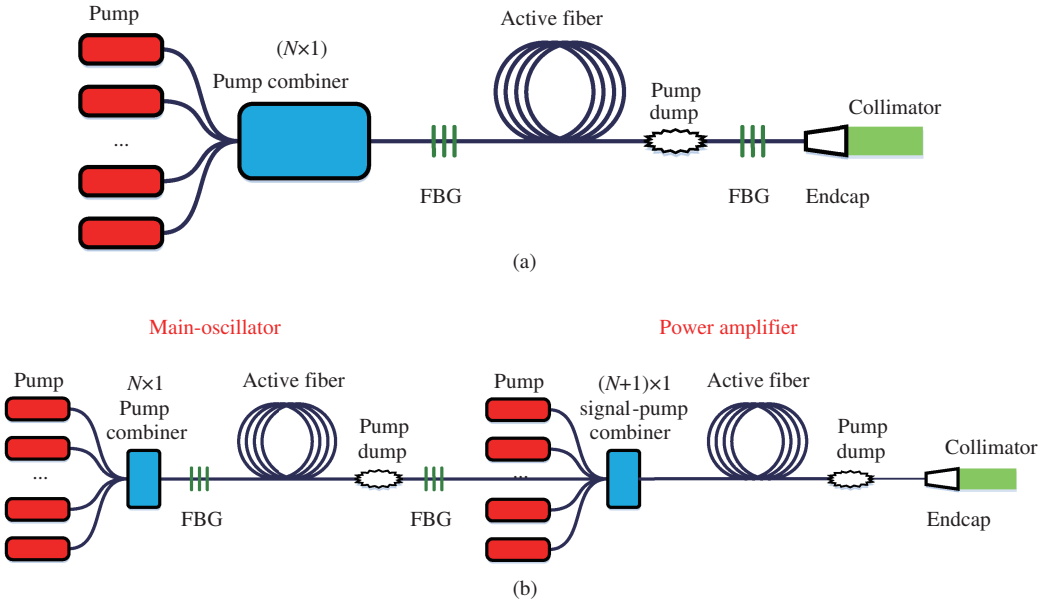

Figure 1 (Color online) Typical setup of fiber laser system. (a) Laser oscillator; (b) laser amplifier.

fiber laser channels could increase the total output power and up to 100 kW fiber laser system has been demonstrated through all-fiber-combiner [16]. Although there are various kinds of technical routes for beam combining [17, 18], only part of them, such as coherent beam combining (CBC) [19] and spectral beam combining (SBC) [20], holds the potential of power scaling while simultaneously maintaining the beam quality. In the past decade, our research group has been investigating on high power fiber lasers and their coherent beam combining [21–30], which would be reviewed at length in the present paper.

2 Enabling technique for fiber laser

There are two mainly categories of fiber lasers, which could be called as bulk-optics based fiber laser and all-fiberized fiber laser. In this paper, we will mainly focus on the latter one because of its compact configuration and flexible operation. Figure 1 denotes a typical system setup of fiber laser, which includes two kinds of mainly categories, that is, laser oscillator and laser amplifier. Despite those classifications, the common techniques that ensure high power operation are almost the same, that is, the pump source, the optical fiber, the passive component (for example pump combiner, endcap, pump stripper, collimator shown in the figure) and nonlinear effects management. Specifically, the optical fiber could be pumped by laser diodes (which is traditional and typical route) or fiber lasers [2]. In this section, we will review and summarize the recent progress on enabling techniques for fiber laser in our group. It is to be noted that laser diode or optical fiber will not be included in this section since we have not investigated them yet for the time being. The fiber lasers that could be used as high-brightness pump source for active fiber would be introduced in Subsection 2.1, various kinds of passive component would be demonstrated in Subsection 2.2, and then techniques for nonlinear effect management would be discussed in Subsection 2.3.

2.1 High brightness pump

The power scaling of fiber lasers is challenged by the brightness of pump sources, nonlinear effects, thermal effects and modal instability [2,11,15]. Tandem pumping technique has been proved to be a useful method to further improve the output power of fiber lasers [6, 12]. Using high-brightness fiber lasers as pump sources, instead of traditional laser diode pumping, could significantly increase the pump brightness and reduce the thermal load. According to the absorption characteristics of various active fibers, fiber lasers operating at proper wavelength could be used as high-brightness pump sources, where the spectral ranges are far beyond the operating wavelength of high-power multimode laser diodes at present time

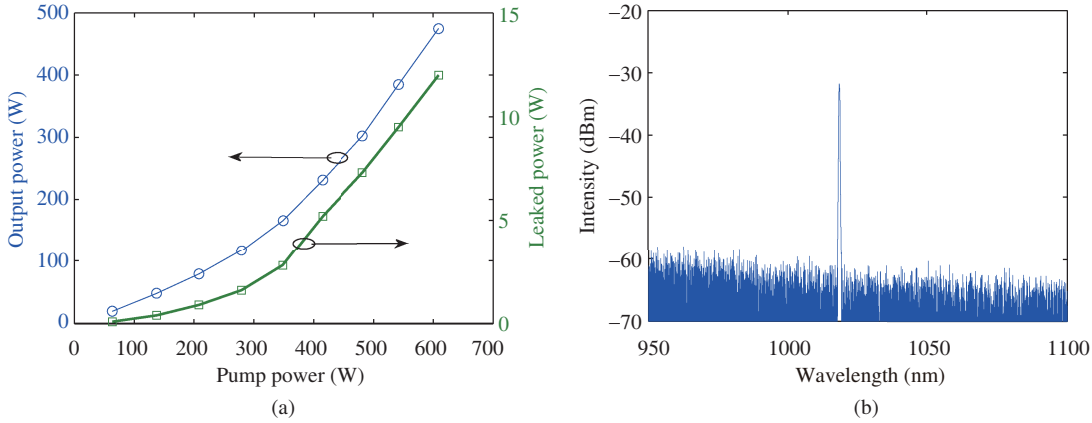

Figure 2 (Color online) Output properties of the 1018 nm fiber laser [33] ©Copyright 2015 Optical Society of America. (a) Output power; (b) optical spectrum at 476 W.

(e.g., 1010–1030 nm for Yb-doped fibers, 1480–1530 nm for Er-doped fibers, 1180/1600/1900 nm for Tm-doped fibers, and 1150/1950 nm for Ho-doped fibers).

Our group has achieved some powerful fiber lasers at some of these specific wavelengths for tandem pumping. For the operating wavelength at 1010–1030 nm, Yb-doped fiber could be employed directly to construct the lasers. However, the laser systems should be designed and optimized carefully to suppress the unwanted parasitic lasing at the common emission band of Yb-doped fiber. In 2012, we demonstrated a 77 W near-diffraction-limited Yb-doped fiber amplifier at 1018 nm with the power conversion efficiency of 75% [31]. In 2013, we reported a 309 W Yb-doped fiber laser at 1018 nm [32]. The power was further improved to 476 W with an efficiency of 78.2% in 2015 based on the Yb-doped fiber with core/inner cladding diameter of 30/250 μm [33], and the output properties of the 1018 nm fiber laser are shown in Figure 2. No sign of power roll-over and amplified spontaneous emission (ASE) can be found during the experiment, which indicates the power was only limited by available pump power. Then several those 500 W-level fiber lasers at 1018 nm were employed as high-brightness pump sources in a tandem-pumped Yb-doped fiber amplifier at 1090 nm to generate laser exceeding 2.1 kW [33]. It is also to be noted that plenty of papers have focused on 1018 nm fiber lasers in past few years [34–39].

We also investigated the power scaling of fiber lasers at 1180 and 1150 nm, which could be employed as the pump sources for Tm- and Ho-doped fiber lasers, respectively. We have carried out the investigations and proof that Yb-doped fiber is capable of lasing at those wavelengths [40, 41]. However, further power scaling of fiber lasers at 1180 nm was achieved based on the Raman gain in passive fibers, due to the small net gain cross section of Yb-doped fiber at this wavelength [42–44]. In 2013, our group demonstrated a 119 W single-mode all-fiber Raman fiber laser at 1173 nm [45], which was core-pumped by a 1120 nm Yb-doped fiber laser. In 2014, we reported a 73.7 W random distributed feedback fiber laser at 1184 nm based on Raman gain [46]. Then in 2016, a record 200 W-level random distributed feedback fiber laser at 1173 nm with the optical efficiency of 89% was achieved by optimizing the fiber length [47].

For fiber lasers operating at 1150 nm, high power laser emission could be directly achieved by a diode-pumped Yb-doped fiber oscillator. By optimizing the length of gain fiber, the parasitic lasing was suppressed and the output power of a monolithic Yb-doped fiber laser reached 120 W with the slope efficiency of 54.5% [48]. In addition to direct laser generation from rare-earth doped fibers, Raman gain and hybrid gain (Yb gain and Raman gain) could also be employed for laser emission at 1150 nm. In 2015, we demonstrated a 100 W-level random distributed feedback fiber laser at 1150 nm based on Raman gain, which was then employed as the pump source of a Ho-doped fiber laser for mid-IR laser generation [49]. To utilize Yb gain and Raman gain simultaneously in the laser cavity, our group constructed a diode-pumped dual-cavity fiber laser at 1150 nm, which was then employed as the pump laser of a dual-wavelength Ho-doped fiber laser [50]. The output power of the hybrid-gain-based fiber laser reached 110.8 W and the parasitic lasing was efficiently suppressed [51]. It is to be noted that this hybrid cavity design has the

potential of lasing at long-wavelength with output power up to kilowatt level [52].

2.2 Passive components

There are various kinds of fiber passive components for assembling a fiber laser, such as pump combiner, pump/signal combiner, fiber Bragg grating (FBG), isolator, circulator, pump stripper, endcap, collimator, and laser combiner. In recent years, we have carried out intensive investigation on kinds of passive components. In this subsection, we would briefly introduce the following four kinds of passive components: pump/signal combiner, endcap/collimator, pump stripper, and laser combiner.

Different types of pump/signal combiners, all-fiber side-pumping combiners, especially using tapered-fused method, appear to have more and more potential in high-power fiber lasers due to its uninterrupted signal fiber core and unlimited pump points [53, 54]. We have studied theoretically and experimentally in detail the fabrication of all-fiber side-pumping combiner [53, 55], fiber amplifier with output power of more than 2.5 kW and slope efficiency of near 83% has been achieved based on the self-made combiner.

High power fiber end-cap is an essential component for high power fiber lasers, the key technique of which is the splicing of fiber end-caps with low loss and high tension strength. Due to the huge difference of the diameters of fiber and large size end-cap, the splicing of them cannot be realized by traditional fusion splicers. A fiber end-cap splicing system has been designed and built in our own lab [56]. In the year of 2016, output power with more than 3 kW was realized with a single-mode fiber end-cap while only heating up by 7°C/kW without active cooling, and output power with 6.08 kW was realized with a multimode fiber end-cap while only heating up by 6°C/kW without active cooling [57]. And in the following years, the power handling of endcap has surpassed 14 kW level [58]. In addition to the endcap, we have also achieved monolithic fiber end cap collimator for high-power free-space usage [59], even beam steering function could be built-in inside the monolithic device [60, 61].

In cladding pumped fiber lasers, there are inevitably cladding light inside the system, the amount could be as much as hundreds of watts. If the cladding light is not filtered properly, it would not only degrade the laser beam quality, but also increase the risk of damaging different components, e.g., collimators [62]. In the year of 2014, an efficient cladding light extracting through cascaded strippers was proposed [62], where a selected part of the fiber is divided into five segments, and the fluoroacrylate jackets of three interval segments are gradually removed and replaced with different higher index polymers. The power-handling capability of the device was tested up to cladding light of power up to 150 W. A high attenuation of 18 dB has been achieved, whereas the maximum local temperature was less than 64°C.

Laser combiner is a passive fiber component based on tapered fiber bundles (TFB) technology [63]. By using several channels of high-beam-quality (for example, single-mode) fiber lasers as the input channel, much higher power with lower-beam-quality (for example, multimode) fiber laser could be achieved, which is beneficial for direct use, for example, manufacturing pump source [64, 65] or direct material processing. Recently, an all-fiber 7×1 signal combiner with an output core diameter of 50 μm have been fabricated, which could enable ∼14 kW output power [58]. The comprehensive test platform for high power laser combiner, fiber endcap and cladding light stripper is shown in Figure 3(a). As shown in Figure 3(a), these devices have been tested using seven single-mode fiber lasers with 2 kW output power at 1080 nm and a total combined power of 14.1 kW could be transmitted with loss of less than 1.5%. The beam quality of the combined beam is measured, which deteriorates little in the power scaling process. At maximal output power, the beam quality of M^2=5.37 is achieved, as shown in Figure 3(b). In the power scaling process, the temperatures of laser combiner and fiber endcap are just heating up by 3°C/kW and 2.5°C/kW, respectively. Despite high power laser combining via laser combiner could be difficult to fulfill effective brightness scaling, it is a simple and efficient approach to achieve high power all-fiberized fiber source for laser processing and laser machining.

2.3 Nonlinear effects management

Nonlinear effects, such as stimulated Brillouin scattering (SBS), stimulated Raman scattering (SRS) and thermal-induced mode instability (TMI) are the primary limitations for brightness scaling of fiber laser

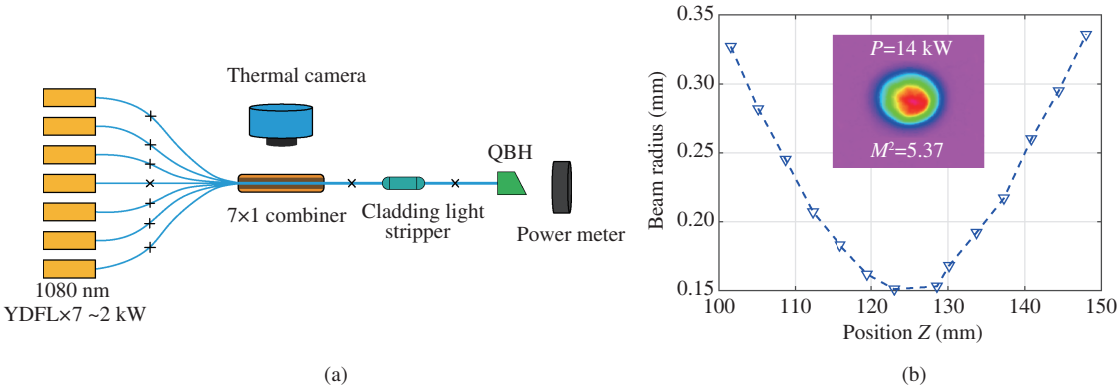

Figure 3 (Color online) (a) The comprehensive test platform for high power laser combiner, fiber endcap and cladding light stripper; (b) the beam quality measurement at maximal output power [58].

systems [14]. The SBS and SRS effects could be regarded as the optical nonlinear effects, which would determine the upper limitation of the power scaling and consequently further limit the brightness scaling. TMI could be regarded as the thermal-induced nonlinear effect, which would impair the beam quality of the transverse mode. As a result, the brightness of fiber lasers/amplifiers would be limited. In the following subsection, the management of different nonlinear effects would be discussed in detail.

2.3.1 *SBS effect*

SBS effect is caused by the interaction between the optical and acoustic fields in optical fibers [66], which is one of the primary limitations in narrow linewidth fiber amplifiers. As for the physical mechanism of SBS effect, the dynamics of SBS in optical fibers without external feedback induced by frequency detuning from resonance had been analyzed by our group [67]. Further, the SBS threshold in multimode fibers with different lengths has been established [68], which provides a more generalized criterion for optimizing the high power, narrow linewidth amplifiers. In recent years, we have successfully fulfilled many SBS suppression methods in high power narrow linewidth fiber amplifiers, including multi-tone injection and amplification [69, 70], using highly doped and short active fiber [28, 71], employing tapered active fiber [72], imposing strain gradients [28], using cascaded sine signal modulation [25] and white noise modulation [73].

2.3.2 *SRS effect*

As for the physical mechanism of SRS effect, most of the studies have been conducted based on the steady-state rate equations together with the power coupling equations [74–76]. By these classical models, analysis shows that SRS threshold in fiber amplifiers is mainly dependent on the fiber structural parameters, such as the effective mode area, fiber length and the transverse distribution of the active fiber core. A main deficiency of the classical models is that the influence of the temporal properties of the injected seed on the SRS threshold could not been considered. Recently, a spectral model by incorporating SRS effect, fiber structural parameters and the temporal properties of the injected seed has been proposed and established by our group [77, 78], and it has been successfully employed to investigate the SRS effect in high power fiber amplifiers seeded by fiber oscillator and narrow-band filtered superfluorescent source. Quite recently, this spectral model has been extended to analyze the intrinsic mechanism for spectral evolution in single-frequency Raman fiber amplifier [79]. Based on our spectral model, except for increase of effective mode area and decrease of the active fiber length, an essential issue to suppress SRS effect is to decrease the temporal instabilities of the injected seed [77, 78]. Based on this consideration, some new SRS suppression strategies have been proposed, such as designing the spectral bandwidths of the high and low reflective gratings in fiber oscillator [77], increasing the output power of the fiber oscillator [77], increasing the filtered bandwidth of the superfluorescent source and so forth [78]. Except for the direct SRS suppression above mentioned, a novel thought to manage nonlinear

SRS effect is to employ this nonlinear effect to generate high power emission from 1120 to 1150 nm based on Yb-Raman fiber amplifiers [80–83]. In this case, the Yb-doped amplifiers are seeded with a pair of Raman wavelengths (for example 1070 and 1120 nm) and the Raman Stokes wave is amplified by Yb-ion gain as well as the Raman gain resulting in more efficient energy transfer [81, 82].

2.3.3 *TMI effect*

The physical principle of TMI is thought to be stimulated thermal Rayleigh scattering [84], which has been firstly explained by Smith et al. in [85]. TMI effect is commonly elaborated by the interaction among optical field, refractive index perturbation field and temperature field. After TMI was firstly observed [86], several theoretical models have been developed to deal with it numerically or analytically [85, 87–90]. Despite that fully numerical model is capable to analysis many TMI characteristics, some aspects of the underlying physics are often lost in the numerical process. Semi-analytical model could be realized at the cost of some accuracy by introducing some approximations, which provides a good understanding of physical insight. As for TMI effect, we propose an improved semi-analytical steady-periodic model in Yb-doped fiber amplifiers [91]. Based on our theoretical model, the influence of fiber parameters (geometric size of the active fiber, V-number, dopant size, photo darkening), characteristics of the seed (fraction of initial higher order modes (HOMs), amplitude modulation, relative intensity noise, output power, emission wavelength, linewidth), parameters of the pump source (amplitude modulation, total pump absorption, pumping wavelength, pumping manner) have been carefully analyzed in detail [92, 93]. Consequently, some strategies to scale the TMI threshold have been proposed [93–95], which could be classified as two types. One type is optimizing the design of the active fiber parameters and the other type is optimizing other essential parts of a fiber laser. As for the first type, the suppression approaches mainly include reducing the core to pump cladding ratio, optimizing the doping area, reducing the V-number, increasing the total pump absorption, suppressing photo darkening. As for the latter type, the suppression methods mainly include increasing the seed power, increasing the linewidth of the seed, lasing at wavelength with larger emission cross-section, pumping at wavelength with smaller absorption cross-section, employing counter/bi-direction pumping manner, employing tandem pumping technique, and increasing the bend loss of HOMs. Further, based on the combination of multiple TMI suppression methods, toward >10 kW laser diode pumped single mode fiber laser system has been designed [93].

3 High power fiber lasers

3.1 Narrow-linewidth fiber laser

High power fiber amplifiers with narrow linewidth and near-diffraction-limited (NDL) beam quality have been found wide applications, such as CBC [17, 23, 96], SBC [97, 98], gravitational wave detection (GVD) [99], nonlinear frequency conversion [100] and so forth. Narrow linewidth fiber amplifiers mainly include two classifications. One is strictly single frequency with the spectral linewidth of within tens of kHz and the other is narrow band with spectral linewidth from GHz to tens of GHz. The main issues for brightness scaling of this type of fiber source are to overcome the detrimental SBS and TMI effects. Besides, it should be pointed out that except for output power and spectral linewidth, linear polarization is also strongly required in many applications of narrow linewidth fiber sources [101]. Notably that the effective Brillouin gain in polarization-maintained (PM) active fiber is typically higher than in non-PM (NPM) fiber, SBS management in high power narrow linewidth and PM amplifiers is more difficult [102]. Further, previous study shows that the TMI threshold in PM fiber amplifiers seems to be remarkably lower than that in NPM fiber amplifiers [103]. Consequently, brightness scaling of narrow linewidth fiber lasers with linear polarization is generally more challenging than the stochastic polarized ones even with the same system parameters. In this section, we would review the development of narrow linewidth fiber laser in our group and then give typical results both here and abroad as a comparison.

As for high power, all fiberized and strictly single frequency fiber amplifiers, we demonstrate an SBS-

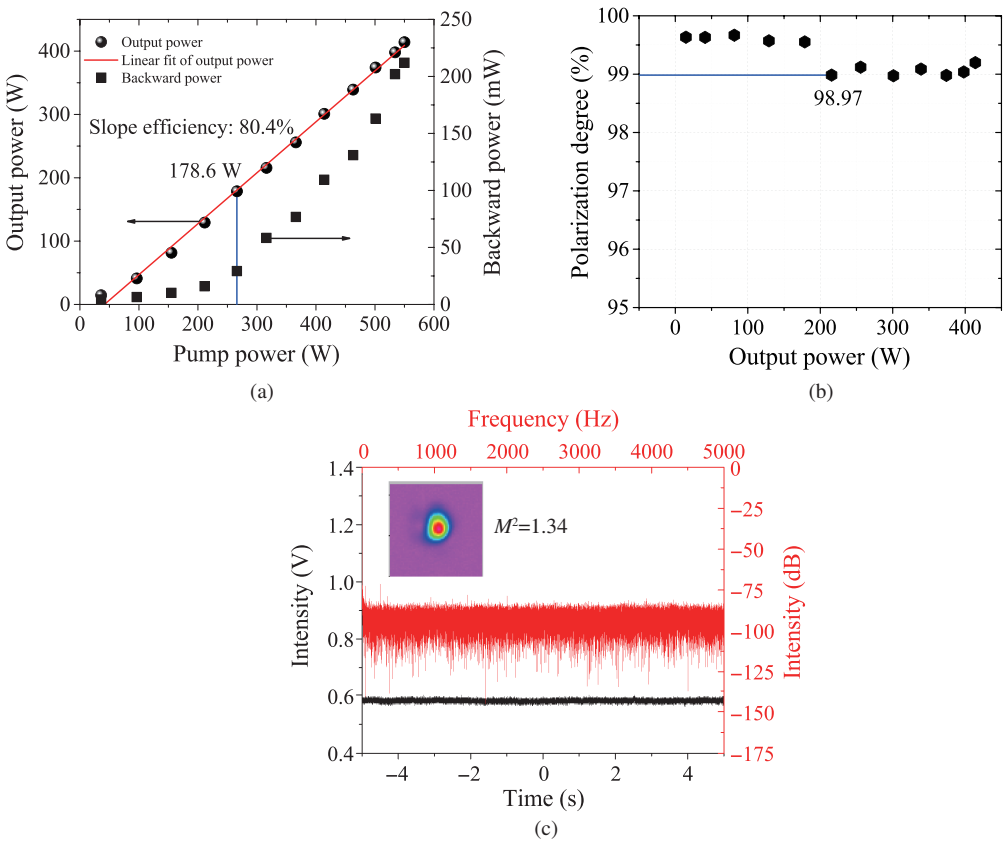

Figure 4 (Color online) Experimental results of the 414 W single-frequency and single-polarization MOPA system [28] ©Copyright 2016 Optical Society of America. (a) Dependence of the output power and backward power on the coupled pump power; (b) dependence of the polarization degree on the output power; (c) temporal trace of the laser at the maximum output power and the corresponding Fourier transform spectrum (the inset is the beam profile at the maximum output power).

limited 168 W configuration with 82.9% power conversion efficiency in 2012 [104]. After that, in order to further mitigate SBS effect, highly doped and short large-mode-area (LMA) active fiber with core diameter of 30 μm and absorption coefficient of 16 dB/m at 975 nm is incorporated into the main amplifier to boost the output power of 310 W with M^2 factor about 1.3 in the same year [105]. A point that should be emphasized is that the polarization states in the aforementioned high power demonstrations are stochastic. In 2013, 332 W all-fiberized and PM amplifier with single polarization (average extinction ratio >21 dB) was presented based on master oscillator power amplifier (MOPA) configuration. SBS suppression could be fulfilled by using just 2.8 m highly doped LMA Yb-doped and PM active fiber with core diameter of 30 μm and cladding diameter of 250 μm [71]. The slope efficiency of the main amplifier was measured to be 83.7% and the beam quality (M^2 factor) is measured to be 1.4 at maximal output power. In the early of 2017, we successfully achieved a 414 W single frequency and single polarization MOPA system by simultaneously using highly doped and short active fiber (with core diameter of 25 μm and cladding diameter of 250 μm) and strain gradients to suppress SBS effect [28]. As shown in Figure 4(a), the slope efficiency of the main amplifier is about 80.4% without observing the SBS effect. The polarization degree is higher than 98% at all power levels (shown in Figure 4(b)). The temporal distribution and its frequency domain at maximal output power are quite stable (shown in Figure 4(c)), which denotes that TMI effect is not emerged in the experiment. At 400 W power-level, the beam quality is measured with an M^2 of 1.34 (shown in the inset of Figure 4(c)).

Table 1 [28,71,105–117] lists the typical research results on single frequency fiber amplifiers within the recently dozen years. As for strictly single frequency fiber lasers, up to 811 W output power has been reported based on free space bulk-components and new fabricated crystal active fiber [106]. Nevertheless,

Table 1 Typical research results on single-frequency fiber amplifiers

Year	Institution	Configuration	Power (W)	M^2	Polarization	Ref.
2005	University of Southampton, UK	Not-all-fiber	264	1.1	PM	[107]
2006	Laser Zentrum Hannover, Germany	Not-all-fiber	148	<1.2	PM	[108]
2007	Corning, USA	Not-all-fiber	502	1.4	NPM	[109]
2007	University of Southampton, UK	Not-all-fiber	402	<1.1	PM	[110]
2007	University of Southampton, UK	Not-all-fiber	511	1.6	NPM	[110]
2008	OFS Laboratories, USA	All-fiber	194	1.2	NPM	[111]
2009	Air Force Research Laboratory (AFRL), USA	Not-all-fiber	260	<1.3	PM	[112]
2011	AFRL, USA	All-fiber	203	–	PM	[113]
2011	University of Michigan, USA	Not-all-fiber	511	1.2	PM	[114]
2012	National University of Defense technology (NUDT), China	All-fiber	310	1.3	NPM	[105]
2012	Laser Zentrum Hannover, Germany	All-fiber	301	1.15	NPM	[115]
2013	Shanghai Institute of Optics and Fine Mechanics (SIOM), China	All-fiber	170	1.02	PM	[116]
2013	NUDT, China	All-fiber	332	1.4	PM	[71]
2014	AFRL, USA	Not-all-fiber	811	<1.2	PM	[106]
2016	Laser Zentrum Hannover, Germany	Not-all-fiber	158	–	PM	[117]
2017	NUDT, China	All-fiber	414	1.34	PM	[28]

as a result of compactness, easy to maintenance and high stability, all-fiberized structures are preferable in the practical application systems. As for all fiberized formats, our 414 W fiber system presented above represents the highest output power with linear polarization and near-diffraction-limited beam quality [28]. It should be noted that despite many efforts from several institutions were made in the past dozen years, as a result of the dual limitations of TMI and SBS, the output power of monolithic single frequency fiber amplifiers has yet not beyond 1 kW at present.

In order to balance the conflict between SBS and TMI, one effective method is to broaden the linewidth of fiber amplifiers from GHz to tens of GHz, which would remarkably enhance the SBS threshold and permit more alternative options of active fiber parameters in the main amplifier for TMI suppression. As for narrow linewidth fiber sources, by using two-tone amplification, we demonstrated a 275 W all fiberized system with power conversion efficiency of 76.6% in the early of 2012 [69]. In the same year, by using sine wave phase modulation, as high as 666 W was presented with spectral linewidth of ∼0.3 GHz and optical to optical conversion efficiency of 86% at maximal pump power [118]. Later, SBS effects prevent further power scaling of the narrow linewidth fiber amplifiers. In 2015, we presented a narrow linewidth, all-fiber and PM amplifiers seeded by a phase-modulated single-frequency laser, which is modulated by simply imposing an excited signal to an acoustic-optical driven source [119]. By amplifying the phase-modulated seed, a 560 W output laser had been achieved with slope efficiency of 87.2%, M^2 ∼1.3, polarization extinction ratio (PER) of ∼14 dB and linewidth of <5 GHz, respectively. Further power scaling is limited by TMI instead of SBS effect. Thus, we aimed to investigate the physical mechanisms and suppressing methods of TMI issue. In the same year, we found that increasing relative mode losses of HOMs by coiling the active fiber is an efficient approach to suppress TMI effect [94], which was quickly validated in a 1.3 kW all-fiberized MOPA system. In 2016, we demonstrated 434 W an all-fiber linear-polarization dual-frequency Yb-doped fiber laser carrying low-noise radio frequency signal [70]. In the same year, we demonstrated high power, all-fiberized and PM amplifiers with narrow linewidth and near-diffraction-limited beam quality by simultaneously suppressing detrimental SBS and TMI effects [25]. The SBS effect was suppressed by using cascaded sine wave signal phase modulation and the TMI was suppressed by coiling the active fiber in the main amplifier. Output power of 1.89 kW was ultimately achieved with a linear-fitting slope efficiency of 74%, PER of ∼15.5 dB and full-width at half maximum (FWHM) of ∼0.17 nm (45 GHz). In 2017, the output power of this system was further scaled to be 2.43 kW by carefully optimizing the coiling structure to suppress TMI and using white noise source (WNS) phase modulation to suppress SBS effects [73]. The typical results are shown in Figures 5(a)–(c). Figure 5(a) shows the output power scaling process along with increase of pump power and the inset

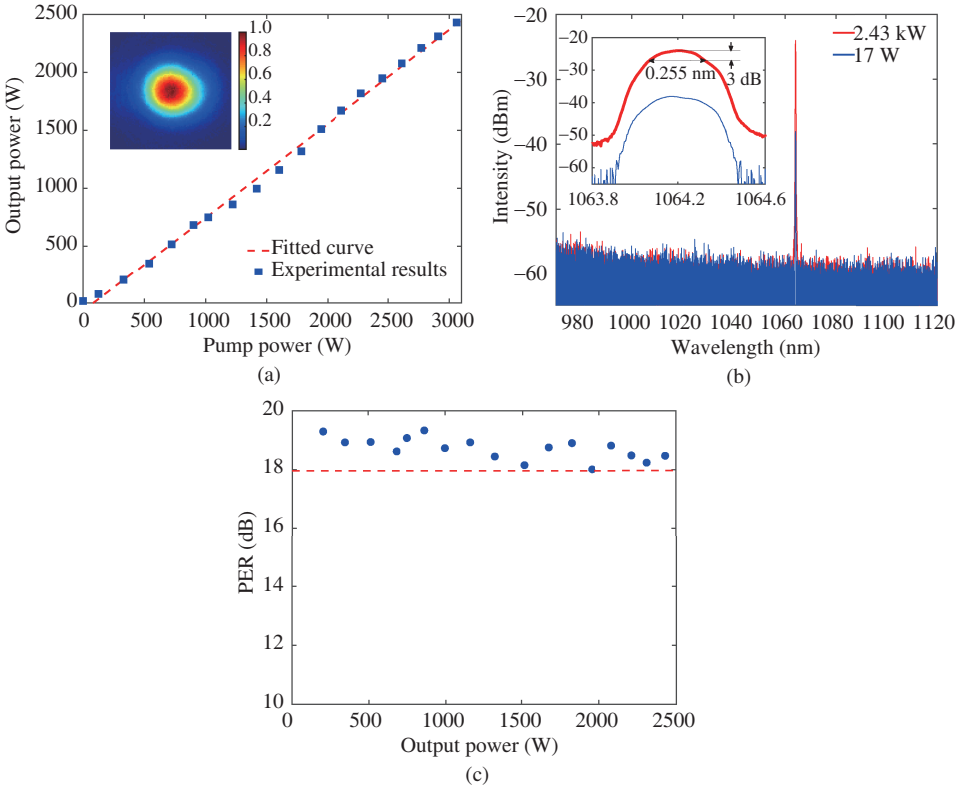

Figure 5 (Color online) Experimental results of the narrow-linewidth near-diffraction-limited all-fiber PM amplifier [73] ©Copyright 2017 Astro Ltd. Reproduced by permission of IOP Publishing. (a) The output power scaling process along with increase of pump power (inset shows the beam profile at 2.43 kW); (b) the spectral distributions at 17 W and 2.43 kW; (c) the measured PER result with increase of output power.

shows the beam profile at maximal output power, which denotes that near linear-dependent relationship could be obtained with near-diffraction-limited beam quality. Figure 5(b) shows the spectral distributions at 17 W and 2.43 kW. The FWHM is measured to be 0.255 nm at maximal output power, which broadens little in the power scaling process. Figure 5(c) is the measured PER result with increase of output power. As shown in Figure 5(c), the PER is also deteriorated little and PER of 18.3 dB is achieved at 2.43 kW.

Quite recently, a record output power of 4 kW-level all-fiberized and narrow-linewidth MOPA system has been demonstrated. The stimulated Brillouin scattering (SBS) effect could be balanced and suppressed by simply using one-stage white noise phase modulation technique. Figures 6(a)–(c) show the power scaling process as a function of pump power, the spectrum and the beam quality (M^2 factor) at maximal output power, respectively. As shown in Figure 6(a), the maximal output power is scaled to be 3.94 kW with linear slope efficiency of 78%. As shown in Figure 6(b), the spectral linewidth account for 90% power is ∼0.89 nm at full power and the signal to noise ratio (SNR) of signal laser is higher than 31.5 dB compared to the pump light. SRS could be suppressed by a factor of ∼24.9 dB, but it would be a challenge for further power scaling. At 3.94 kW, the beam quality is measured to be M^2 ∼1.86 (shown in Figure 6(c)).

Table 2 [25,73,103,120–135] lists the typical research results on narrow linewidth fiber amplifiers within the late decade. From Table 2, it is shown that the output power of narrow linewidth fiber amplifier had been beyond 1 kW in 2008 by Nufern. As for stochastic polarized ones, the output power was scaled to ∼3.5 kW with linewidth of ∼47.4 GHz based on free space bulk-components and low NA active fiber in 2017 [120]. Further, as high as 3.5 kW output power with linewidth of ∼0.175 nm had been reported in all-fiberized format in 2018 [121]. To the best of our knowledge, the 4 kW level output power performed by our group is the highest power-level emitted from narrow-linewidth fiber laser system at present. As for linear-polarized one, <3 kW output power had been achieved in metalized Yb-fiber amplifier (not-all-

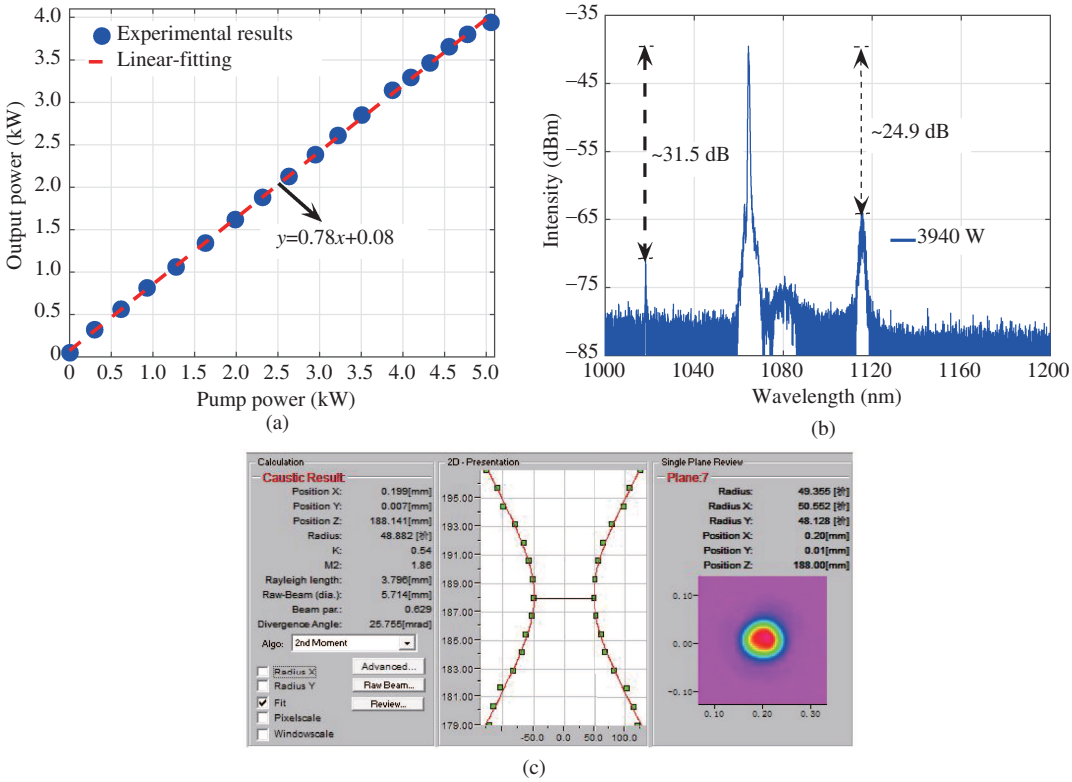

Figure 6 (Color online) Experimental results of the 4 kW-level narrow-linewidth fiber laser system. (a) The power scaling process as a function of pump power; (b) the spectrum at maximal output power ©Copyright 2018 Cambridge University Press; (c) the beam quality at maximal output power ©Copyright 2018 Chinese Laser Press.

Table 2 Typical experimental results on narrow-linewidth fiber amplifiers

Year	Institution	Configuration	Power (kW)	M^2	Linewidth	Polarization	Ref.
2008	Nufern, USA	All-fiber	1.01	<1.25	8 GHz	PM	[124]
2010	Northrop Grumman, USA	All-fiber	1.43	–	25 GHz	PM	[125]
2014	Nufern, USA	All-fiber	1.50	–	–	PM	[126]
2014	Lockheed Martin, USA	All-fiber	1.14	1.08	12 GHz	PM	[103]
2014	AFRL, USA	All-fiber	1.17	1.2	3 GHz	NPM	[127]
2015	IPG Photonics, USA	All-fiber	>1.5	1.1	<15 GHz	NPM	[128]
2015	Shandong HFB Photonics, China	All-fiber	2.05	<1.4	75 GHz	NPM	[129]
2015	University Jena, Germany	All-fiber	2.3	<1.3	45 GHz	NPM	[130]
2015	MIT Lincoln Lab, USA	Not-all-fiber	2.55	<1.15	<12 GHz	NPM	[131]
2015	IPG Photonics, USA	All-fiber	1.03	1.18	20 GHz	PM	[132]
2016	NUDT, China	All-fiber	1.89	<1.3	45 GHz	PM	[25]
2016	MIT Lincoln Lab, USA	Not-all-fiber	3.1	<1.15	12 GHz	PM	[122]
2016	University Jena, Germany	Not-all-fiber	3	1.3	0.17 nm	NPM	[133]
2016	AFRL, USA	All-fiber	1	1.2	2.5 GHz	NPM	[134]
2017	NUDT, China	All-fiber	2.43	–	0.255 nm	PM	[73]
2017	University Jena, Germany	Not-all-fiber	3.5	1.3	47.4 GHz	NPM	[120]
2018	China Academy of Engineering Physics	All-fiber	3.5	1.9	0.175 nm	NPM	[121]
2018	IPG Photonics, USA	All-fiber	2	1.1	30 GHz	PM	[123]
2018	IPG Photonics, USA	All-fiber	2.5	1.1	30 GHz	NPM	[123]
2018	nLight Photonics, USA	All-fiber	2.6	–	20 GHz	NPM	[135]
2018	NUDT, China	All-fiber	3.94	1.86	0.89 nm @90% energy	NPM	–

fiber) with spectral linewidth of 12 GHz and near single mode operation [122]. The output power record directly extracted from all-fiberized polarization-maintained fiber amplifier is 2.43 kW, which was fulfilled

by our group in 2017 [73]. Besides, active polarization control technique could be used to generate the linear-polarized output from non-polarization-maintained fiber amplifiers, and as high as 2 kW output power had been performed in all-fiberized format quite recently [123].

3.2 Broadband fiber laser

High power broadband fiber lasers could be used in plenty of application fields where there is no requirement on the laser linewidth such as cutting and welding. Just like other kinds of high power lasers, there are mainly two technical categories to achieve high power fiber laser, that is, laser oscillator and laser amplifier. Our group have focused on investigation on both high power fiber laser oscillators and amplifiers [8, 33, 81, 101, 136–146], which would be reviewed in the following paragraphs.

As for high power fiber oscillator, in 2014, we demonstrated a fiber laser oscillator with a maximum output power of 1.5 kW pumped by 915 nm laser diode, which was limited by the stimulated Raman scattering (SRS) effect [137]. After that, we mitigated the SRS effectively by employing short gain fiber together with the bidirectional 976 nm laser diode pumping scheme [138–140], a maximum output power of 3.05 kW was achieved with a Raman stokes suppression of ∼29 dB. Theoretically, SRS can be further mitigated by decreasing gain fiber length or increasing fiber mode area. Nevertheless, it seems not too straightforward since decreasing gain fiber length or increasing fiber mode area will help the generation TMI [93]. In late 2017, we successfully realized a high power monolithic fiber laser oscillator with a maximum output power of 5.2 kW based on a trade-off design between the SRS and TMI. The laser oscillator was built with Yb-doped fiber with core/inner cladding diameter of 25/400 μm and corresponding home-made FBG. The bidirectional pump scheme employing 915 nm laser diode could help to increase the TMI threshold [91, 95], while the SRS was mitigated by employing large mode area fiber and optimizing bidirectional pump distribution. The monolithic fiber laser oscillator could be scaled up to 5.2 kW with slope efficiency of ∼63%, as shown in Figure 7(a). The intensity of the Raman stokes light is ∼22.3 dB below the signal laser (shown in Figure 7(b)) and the beam quality (M^2 factor) is measured to be ∼2.2 (shown in Figure 7) when the laser operates at full power level.

Table 3 [137, 139–141, 147–154] lists the typical research results on directly broadband fiber oscillator, which shows that 2017 seems to be a memorable year. Before 2017, the maximal output power from all-fiberized broadband fiber oscillator was 2.5 kW [139]. At the beginning of 2017, Ikoma et al. reported the first 3 kW monolithic all-fiberized laser oscillator [147]. At the mid and late of 2017, 4 kW output power was demonstrated [141, 155]. Nowadays, the extracted output power from directly fiber oscillators has been beyond 5 kW power level [148, 149], which could provide a prominent progress of output power scaling via high power signal combiner shown in Subsection 3.2.

At earlier time, our group focused on fiber amplifier pumped by commercially available laser diodes (LDs) [81, 136, 142, 143]. Then it is gradually found that power scaling of fiber amplifiers in the lab is limited by the brightness of laser diode, and also the newly observed but not resolved TMI issue. Pumping active fiber by using fiber lasers (tandem pumping), might simultaneously solve the brightness [12] and TMI issue [91, 93, 95]. So in recent years, we also have emphasized on high power fiber amplifiers based on tandem pumping technique [33, 144, 146]. In [144], we have successfully achieved a 3.5 kW fiber amplifier based on tandem pumping. The slope efficiency is as high as 87.5% because of the low quantum defect [156], which would inherently help to suppress the TMI effect because of much less heat generation. It is to be noted that the active fiber was pumped by 24 channels of fiber lasers that exceed of the typical pump channels for laser diodes (for example, 6 channels for single-end pumping), which could be attributed to the brightness of the fiber laser pump because of the brightness-conservation law. Based on tandem pumping scheme, we have further successfully built the first 10 kW fiber laser with good beam quality in China [157]. Figures 8(a) and (b) show the power scaling process and the far-field beam profile of the fiber laser system, respectively. With the total injected 1018 nm pump power of 12.1 kW, as high as 10.1 kW output power has been achieved with optical to optical conversion efficiency of ∼83.4%. At maximal output power, the beam quality (BQ) is measured to be ∼1.95.

Table 4 [83, 120, 136, 157–165] lists the typical research results on high power broadband fiber amplifiers.

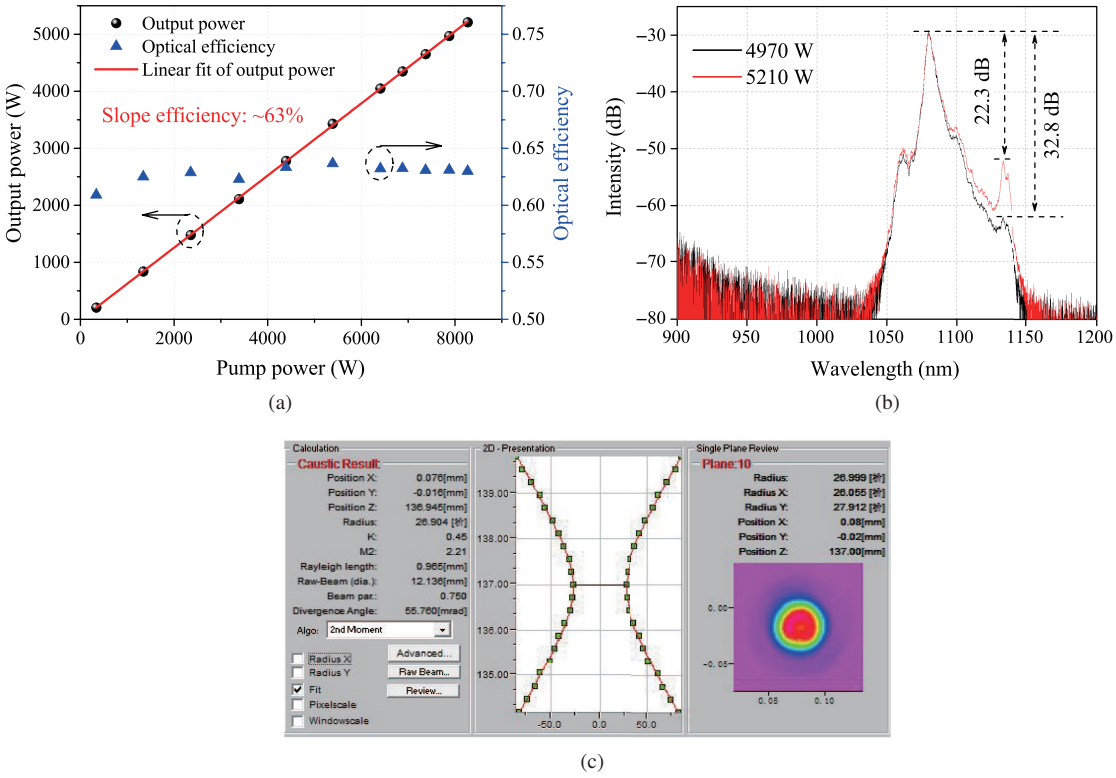

Figure 7 (Color online) Output properties of the 5.2 kW monolithic fiber laser oscillator [145] ©Copyright 2018 Chinese Laser Press. (a) Output power and optical efficiency; (b) optical spectra at 4970 and 5210 W; (c) beam quality of the monolithic fiber laser oscillator at 5.2 kW.

Table 3 Typical research results on directly broadband fiber oscillator

Year	Institution	Configuration	Power (kW)	M^2	Ref.
2012	Alfalight Inc., USA	All-fiber	1	–	[150]
2012	JDSU Inc., USA	All-fiber	1.2	<1.2	[151]
2012	Rofin, Germany	All-fiber	2	1.3	[152]
2014	NUDT, China	All-fiber	1.5	<1.2	[137]
2014	Coherent Inc., USA	Not-all-fiber	3	<1.2	[153]
2016	Fujikura Inc., Japan	All-fiber	2	1.2	[154]
2016	NUDT, China	All-fiber	2.5	1.3	[139]
2017	Fujikura Inc., Japan	All-fiber	3	1.3	[147]
2017	NUDT, China	All-fiber	3	1.3	[140]
2017	NUDT, China	All-fiber	4	2.2	[141]
2018	Fujikura Inc., Japan	All-fiber	5	1.3	[148]
2018	NUDT, China	All-fiber	5.2	2.2	[149]

It is shown that several independent groups have reported their high power fiber lasers with more than 3 kW output power. The highest output power is still ~20 kW reported by IPG Photonics in 2013. Notably that the output power of broadband fiber amplifiers in China developed quickly during the previous five years and higher than 10 kW output power had been successively demonstrated by using tandem pumping (TDP) and laser diode pumping (LDP) manners, respectively [157–159].

3.3 Fiber laser at 2 μm

Fiber lasers operating at 2 μm have many applications [166,167] in the fields of lidar [168], medicine [169, 170], material processing [171, 172], etc. They are promising high-brightness pump sources to generate mid-IR laser emission [173–176]. It is notable that 2 μm fiber lasers have potentials in power scaling,

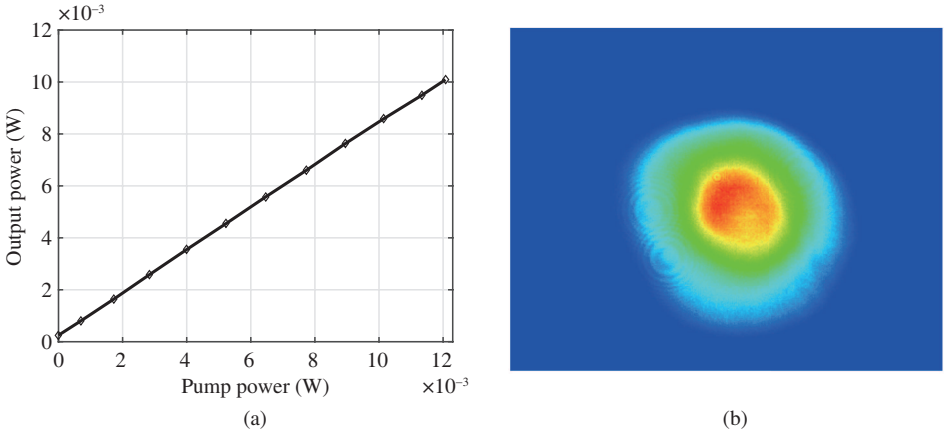

Figure 8 (Color online) (a) The power scaling process of the 10 kW-level fiber laser system; (b) the far-field beam profile at maximal output power [157].

Table 4 Typical research results on high power broadband fiber amplifiers

Year	Institution	Configuration	Pump manner	Power (kW)	BQ	Ref.
2013	IPG Photonics	–	TDP	20	–	[160]
2015	NUDT, China	All-fiber	LDP	3.15	1.6	[136]
2016	Tsinghua University, China	All-fiber	LDP	3.89	–	[83]
2016	Huazhong University of Science and Technology, China	All-fiber	LDP	3	1.3	[161]
2016	China Academy of Engineering Physics, China	All-fiber	LDP	5.07	2.3	[162]
2016	NUDT, China	All-fiber	TDP	10.1	1.95	[157]
2017	University Jena, Germany	Not-all-fiber	LDP	4.3	1.2	[120]
2017	Tianjin University, China	All-fiber	LDP	5	1.7	[163]
2017	Tianjin University, China	All-fiber	LDP	8	<4.3	[163]
2017	Huazhong University of Science and Technology, China	All-fiber	LDP	3.7	–	[164]
2018	China Academy of Engineering Physics, China	All-fiber	LDP	11.23	–	[158]
2018	Tsinghua University, China	All-fiber	LDP	6	–	[165]
2018	China Academy of Engineering Physics, China	All-fiber	LDP	10.6	–	[159]

benefiting from the higher nonlinear effect threshold than that of fiber lasers operating at shorter wavelengths. Based on the Tm^{3+} and Ho^{3+} ions doped in silica fibers, 2 μm fiber lasers have attained kW-level high-brightness laser emission around a decade ago [177–181]. Afterwards, however, the progress of high-power 2 μm fiber lasers were stuck in the underdeveloped pump sources [182] and moderated optical efficiency [183], and the power record stopped at 1 kW level. In these years, researchers have paid their attentions on the tandem pumping technique to further power scale fiber lasers at 2 μm [184–188]. It is indicated that tandem pumping technique could dramatically improve the optical efficiency and significantly reduce the thermal load [189]. Researchers have also made breakthroughs in fiber fabrication to generate 2 μm fiber lasers efficiently [190–192].

For high-power Tm-doped fiber lasers, our group started the research based on commercially-available pump sources, i.e., multimode laser diodes at 793 nm, which is the most commonly used pumping scheme now. We demonstrated a 102 W monolithic single-frequency Tm-doped fiber amplifier at 1971 nm in 2013 [193], then the output power was improved to 310 W in 2015 by optimizing the system and increasing launched pump power [194]. The experimental results including output power, optical spectra measured by an optical spectra analyzer and a scanning Fabry-Perot interferometer are shown in Figure 9. In 2015, we reported a 105 W ultra-narrowband nanosecond pulsed Tm-doped fiber amplifier, in which the linewidth of pulsed seed laser was broadened from ∼24 to ∼307 MHz to increase the stimulated Brillouin scattering threshold [195]. We also demonstrated a 238 W high-average-power nanosecond pulsed Tm-doped fiber amplifier with the maximum peak power of 12.1 kW and the pulse energy of 0.749 mJ [196]. Based on the high-power Tm-doped fiber amplifier, we investigated the power scaling of 2 μm ASE with

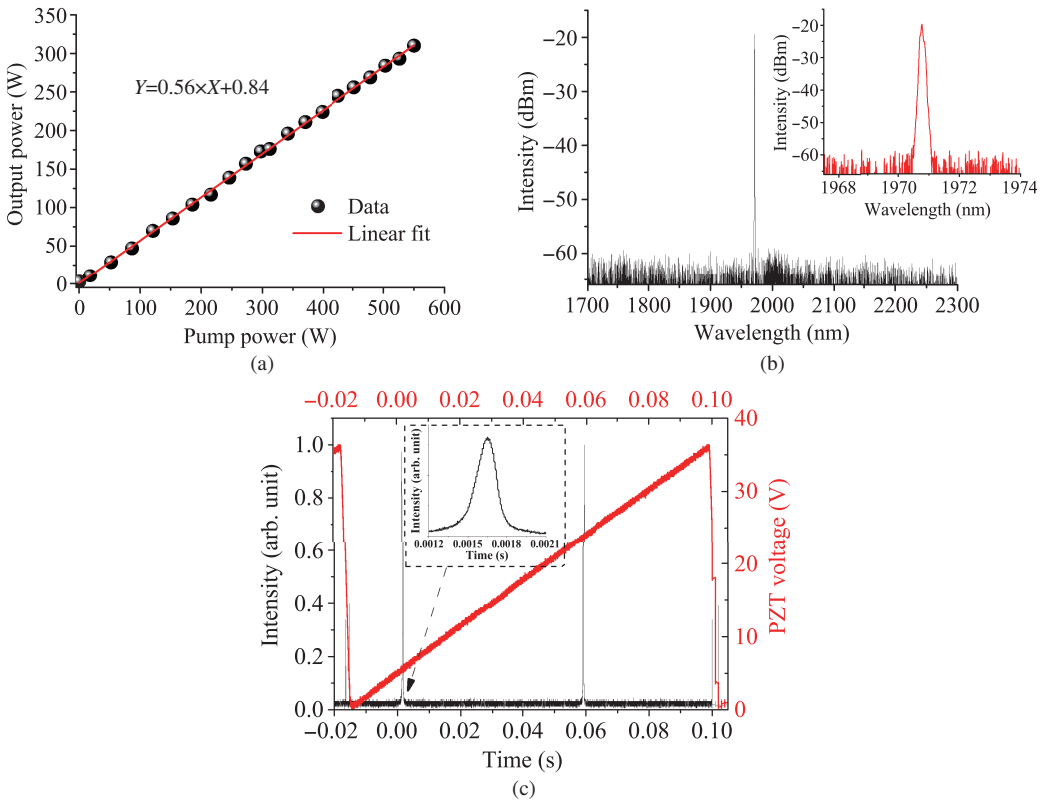

Figure 9 (Color online) Experimental results of 310 W single-frequency Tm-doped all-fiber amplifier [194] ©Copyright 2015 IEEE. (a) Output power; (b) optical spectra (Inset: zoomed-in spectrum); (c) spectrum measured by a scanning Fabry-Perot interferometer to verify the single-frequency operation.

different linewidths. In 2015, we achieved a 316 W broadband ASE sources with a 3 dB bandwidth of 24 nm [197], a 228 W ultra-narrowband ASE sources with a 3 dB bandwidth of 0.19 nm [198] and a 250 W widely tunable narrowband ASE sources with a running range of 35 nm [199].

In addition to multimode laser diode pumping, our group also investigated the tandem pumping technique for powerful 2 μm fiber laser generation. Based on our previous achievements in high-power fiber sources at 1 μm, such as long-wavelength Yb-doped fiber lasers, Raman fiber lasers and random fiber lasers, we employed those homemade powerful fiber lasers as pump sources in Tm- and Ho-doped fiber lasers. In 2014, we reported a 100 W-level Tm-doped fiber laser at 1943 nm [186] cladding-pumped by two homemade high-power 1173 nm Raman fiber lasers [45]. In the same year, our group demonstrated a 42 W Ho-doped fiber laser at 2049 nm [200] core-pumped by a homemade 1150 nm Raman fiber laser. Tandem pumping technique could also benefit long-wavelength fiber laser generation (e.g., >2.15 μm). In 2016, we improved the output power of 2153 nm Tm-doped fiber from 2 W (for 793 nm laser diode pumping) to 18 W (when pumped by a 1173 nm fiber laser) [201]. A home-made high-power random fiber laser at 1173 nm was used as the pump source [47], which could suppress the ASE and parasitic lasing successfully. Recently, we have constructed a high-efficiency ultrafast Tm-doped fiber amplifier tandem-pumped by a continuous-wave fiber laser at 1940 nm [188]. The slope efficiency of the fiber amplifier reached 87%, which is much higher than that of 793 nm pumping scheme (typical value ∼50%) [166,193]. The output power and measured pulse train are depicted in Figure 10. Tandem pumping could dramatically reduce the thermal load when proper pump wavelength used, which also reveals this technique may provide a new avenue for 2 μm fiber lasers when the power is high enough that TMI becomes a physical limit for power scaling [202, 203]. Besides, we had concluded the progress of powerful 2 μm silica fiber sources in the past decades, which could be found in [27].

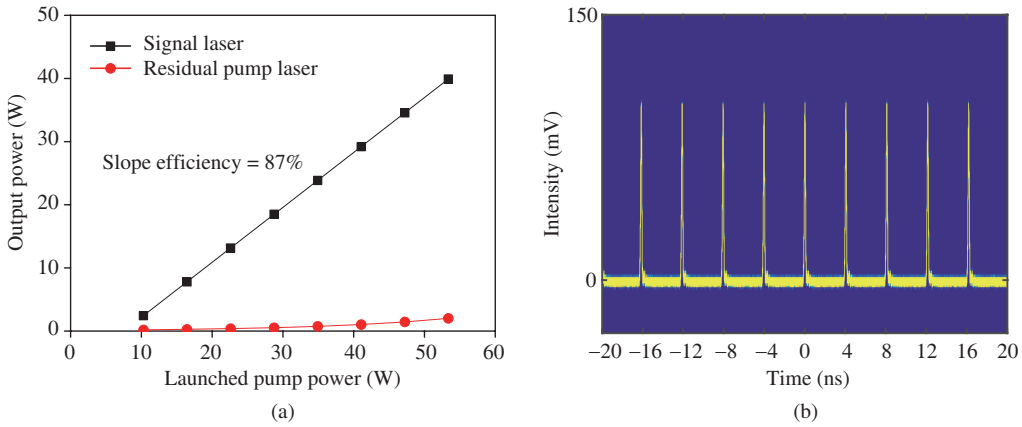

Figure 10 (Color online) Experimental results of the high-efficiency ultrafast Tm-doped fiber amplifier based on tandem pumping [188] ©Copyright 2018 Optical Society of America. (a) Output power; (b) measured pulse trains with a repetition rate of 248 MHz.

4 Enabling technique for CBC

4.1 Phase control

Phase noises exist in fiber lasers/amplifiers because of thermal effects, external environment disturbances and so on. Timely phase control is the key for effectively coherent beam combining. Phase control techniques can be briefly classified into two categories: passive phase control and active phase control. In passive phase control techniques, self-phase locking is realized based on energy coupling mechanisms [204–209] or nonlinear effects [210, 211]. However, the coherent brightness gain saturates at 8–12 elements for passive CBC fiber arrays [212]. In active phase control techniques, feedback control systems are employed to equalize the optical phases of individual fiber lasers. Coherent combining of fiber arrays with kilowatts output power [21, 213–217] and tens of fiber lasers [218–220] have been realized based on active phase control.

Most active phase control CBC systems were based on MOPA configuration, where a single master oscillator (MO) seeds an array of power amplifiers. The phases of the amplifiers are locked and the beams from the amplifiers are effectively combined. Various methods for active phase control have been demonstrated. Those techniques can also be classified into two categories: direct detection and indirect detection. In direct detection techniques, phase errors between amplifiers are directly measured and corresponding phase corrections are implemented timely. Phase measurement approaches such as interferometric measurement [218, 221, 222], Hänsch-Couillaud detection [223, 224] and heterodyne detection [225, 226] have been demonstrated. However, in order to detect phase errors among individual channels, the phase control system is always very complex for ensuring high control band width. In indirect detection techniques, the combined power in the far-field central lobe is maximized based on optimization algorithms such as stochastic parallel gradient descent (SPGD) algorithm [227–229], multi-dithering [216, 217, 230] and single-frequency dithering techniques [21, 231]. In such a system, only one photoelectric detector is used to monitor the combined power in the far-field central lobe. So the system is relatively simple. It is to be noted that in indirect detection techniques, the control bandwidth decreases obviously as the increasing of the number of laser channels. In order to increase the control bandwidth, we proposed code division multiple access (CDMA) based single-frequency dithering technique [232] and cascaded phase control technique [233, 234].

4.2 Tip-tilt control

In the CBC system, tilt-tip error of fiber lasers will also impact the combining efficiency. The tilt-tip error is mainly induced by the limited precision of assembling, beam thermal dithering, vibrations of mechanism, atmosphere perturbations and so on. The mainly used tilt-tip control instruments include

fast steering mirror [235, 236] and adaptive fiber-optics collimator (AFOC) [237–239]. Compared with other tilt-tip control devices, AFOC has the advantages of precise control, small inertia and convenience for packaging. In an AFOC, tip/tilt-control is realized by adjusting the X-direction and Y-direction of the fiber optics output, which located in the focal plane of a lens. The collimated output is deviated on an angle of $\Delta x/f$, where Δx is the traveled distance of fiber optics output in X-direction, f is the focal length of the lens. The tip of fiber optics output is always fixed in the central hole of a cross beam, and adjusting of the fiber optics output is based on four bimorph actuators, two of them drive the X-direction and another two drive the Y-direction [240]. However, the AFOC mentioned above was designed to directly drive the fiber tip, which is not convenient for high power applications. In high power CBC systems, coreless endcaps are usually employed to avoid fiber facet damage. We have designed a novel AFOC based on flexible hinges, which control the fiber end cap instead of the bare fiber [60, 61, 241, 242].

4.3 Aperture-filling

In CBC system, aperture filling is the key technique to achieve high degree of power concentration and excellent beam quality. Aperture filling techniques can be classified into two categories, i.e., divided-aperture coherent combining and coaxial combining. In the tiled-aperture coherent combining system, the combined beam in near field still contains multiple independent sub apertures. The optimal effect of this structure could be equivalent to a large-aperture output, thus to obtain stable interference effect in the far field. In coaxial combining, all the sub beams will be combined into one single laser beam both in the near field and in the far field. As for divided-aperture coherent combining, one common method to aperture filling is based on transmission-type beam splicing in which all the coherently combined beams are arranged in a specific spatial layout. The specific spatial layout could be fulfilled by direct splicing by collimator [243], splicing by micro-lens array [213], etc. The other method to aperture filling is based on reflection-type beam splicing in which the reflectors are employed to reflect all the beams in multi-folds to make beam splicing to improve the fill factor. In this case, beam splicing approaches include discrete reflector splicing [244], platform pyramid splicing [245], step-like beam splicing [246] and so forth. For coaxial combining, aperture filling could be achieved by diffractive optical element (DOE) [247, 248], re-imaging waveguide [249, 250], polarization beam combiners (PBCs), i.e., coherent polarization beam combining (CPBC) [251, 252], high power fiber couplers [208, 253], photonic lantern [254] and so forth.

4.4 Defocus

In CBC system, when fiber laser delivered by fiber endcap, collimated by collimator and projected and combined by other free space components, it is inevitably to induce thermal lens effect at high power density situations. Thermal effect will destroy the wavefront consistence among different channels and cause the decrease of combining efficiency and beam quality. In practical system, the influence of thermal effect on the CBC system could be easily observed by comparing the discrepancies of positions and widths among different beams at far field. In this case, thermal lens compensation is strongly required. As for one of the channels in high power CBC system, by regarding thermal accumulations of all the transmitted components as a unity, the equivalent thermal lens will be effectively suppressed by optimizing the equivalent focus of the fiber collimator. Besides, at different power density, the influence of equivalent thermal lens will be different. Thus, it is advisable to design and employ focus adjustable collimators to compensate thermal lens effect in high power CBC system.

4.5 Optical path difference control

Besides the aberrations mentioned above, combining efficiency also suffers from optical path difference (OPD) [255]. Firstly, OPD will induce the group-delay mismatch. When the phases of two laser beam for the central frequency (ω_0) are locked, the spectral phase shift at frequency of ω_1 is $\Delta\phi_{GD}(\omega_1) = \Delta L(\omega_1 - \omega_0)/\mathrm{c}$, where ΔL is the OPD and c is the velocity of light in the vacuum. Secondly, for a pulsed CBC system, the OPD reduces temporal overlap of the pulses, the time difference of two combined pulses is $\Delta t = \Delta L/\mathrm{c}$. The combining efficiency is influenced mainly by reduction of temporal overlap of the

pulses when CBC of lasers with very narrow bandwidth, and group-delay mismatch becomes the primary factor as the increasing of spectral bandwidth. For pulses with pulse width of 3 ns, the limitation is not temporal overlap but spectral phase when spectral bandwidth is broader 1 GHz [255]. For another example, the OPD must be controlled in $\sim \pm 14$ μm to achieve a combining efficiency of above 95% for combining two ultrashort laser pulses with a spectral bandwidth of 13 nm [256]. It is to be noted that for pulsed CBC system, fiber length difference will induce a phase difference due to self-phase modulation (SPM) and group velocity dispersion (GVD), which will also reduce the combining efficiency. Effective OPD control is helpful for eliminating the influence of SPM and GVD [256, 257].

The mainly used OPD control techniques include spatial optical path adjustment [258], splicing passive fiber [22, 259], and using fiber delay line [213, 260]. Passive fiber and fiber delay line can be employed in all-fiber configuration system, and provide a compact solution. We can compensate very long OPD by splicing passive fiber with a precision of less than 10 mm, which is enough for CW and nanosecond fiber laser with GHz linewidth [255]. For CBC fiber lasers with broader linewidth, fiber delay line can be employed and resolution of less than 1 μm can be obtained [260].

5 High power CBC system

5.1 Tiled CBC

5.1.1 *CW tiled CBC*

In order to confirm the feasibility of CBC techniques such as phase control technique, aperture-filling technique, power scaling technique, we have built a range of CBC systems. In those systems, active-passive hybrid phase control technique [261] and single frequency dithering phase control technique [231] were proposed, novel beam combiner was invented for aperture filling [262], and CBC of multi-tone fiber amplifiers was demonstrated for the first time [263]. In 2010, we built the first CBC system with overall output power of kW level [21], which would be demonstrated and discussed in detail.

The experimental setup is shown in Figure 11. A narrow linewidth seed laser is pre-amplified to 300 mW and split into nine channels. Each channel is coupled to a phase modulator and then amplified by a three-stage all-fiber amplifier. The laser beams from the third-stage amplifiers are spatially coupled via nine collimators, and then tiled using free-space mirrors side by side in a 3×3 laser array. The overall output power of the combined beam could reach 1080 W. Less than 0.1% of the combined beam is sampled for the beam quality diagnosing and phase controlling. As shown in Figure 12, when the control system is in open loop, the phases of the laser beams randomly fluctuate due to phase fluctuation in each fiber channel, which is induced by amplifier temperature variations and environmental disturbances. The normalized energy collected by the pinhole fluctuated between 0 and 0.5 randomly and the intensity pattern observed by the charge-coupled device (CCD) kept shifting. However, when the frequency dithering technique based phase control system is in closed loop, the energy collected by the pinhole can be locked steadily to be more than 0.8 for most of the time. The intensity pattern at the observing plane is clear and steady. By calculation, the fringe contrast of the long-exposure far-field intensity distribution could be more than 85%.

5.1.2 *Pulsed tiled CBC*

Comparing with CW laser CBC systems, some preconditions have to be fulfilled for CBC of pulsed lasers. Firstly, the operation of the actively phase control needs a feedback signal independent of the pulse itself. In pulsed laser CBC systems, the intensity of the combined beam is also influenced by the temporal character of the pulse chain. When the repetition rate of the pulsed laser (f_{RR}) is higher than the phase noise frequency (f_{N}), a low pass filter (LPF) with cut-off frequency of between f_{N} and f_{RR} can be used to eliminate the impact of pulse chain on phase control [233]. For phase control of pulses with lower repetition rate, more complex technique should be employed [264]. Secondly, combining efficiency suffers from additional aberrations induced by temporal mismatch and nonlinear effects, which should

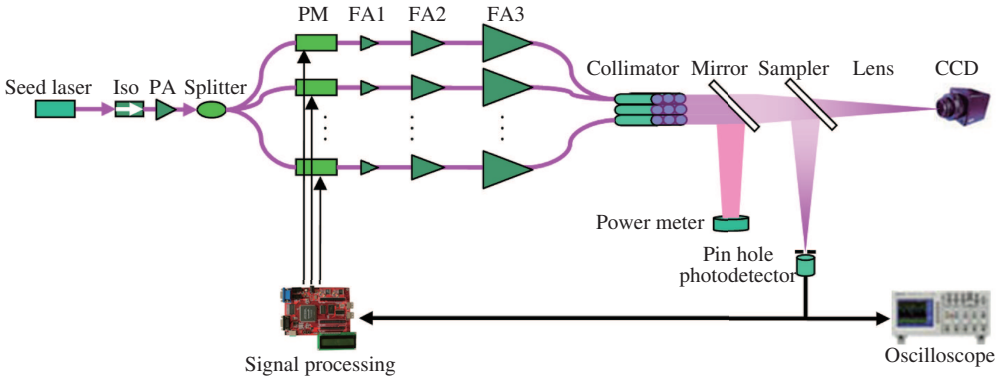

Figure 11 (Color online) Experimental setup of the kW-level CW CBC system ©Copyright 2011 Optical Society of America. Iso: isolator; PM: phase modulator; PA: pre-amplifier; FA: fiber amplifier.

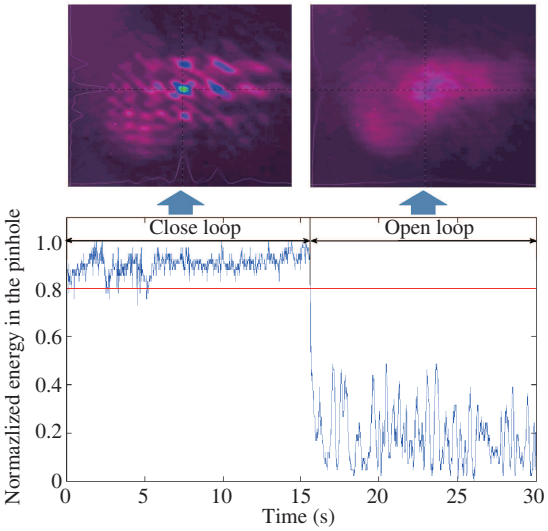

Figure 12 (Color online) Experimental results of CBC of nine CW fiber lasers ©Copyright 2011 Optical Society of America.

be precisely controlled in pulsed CBC systems. We have coherent combined pulsed fiber lasers based on passive [265, 266] and active phasing [22, 258], maximum average power of 1.2 kW was obtained [259]. This system would be demonstrated in this section.

Figure 13 shows the experimental setup, which is similar to the CW one as shown in Figure 11. The differences are as follows. Firstly, the laser seed is generated by directly modulating a single-frequency CW laser using an electro-optic modulator. Secondly, passive fibers with suitable lengths are spliced in the laser channels. In our experiment, a mode-locked laser with pulse width of ∼100 ps is used as the probe to measure the delay time Δt between pulses. OPD can be calculated and a passive fiber with length of $c\Delta t/n$ is spliced in the channel with shorter optical path, where n is the refractive index of the fiber core. Thirdly, in order to eliminate the fluctuation caused by pulses with a repetition rate of 5 MHz, a low pass filter with a bandwidth of ∼3 MHz is connected to the PD.

When the phases of the laser amplifiers are locked, the normalized intensity detected from the pinhole could be steadily more than 0.9 most of the time, and the contrast of the long-exposure far-field intensity pattern of the coherently combined beam could increase from approximately zero to 89.1 %, as shown in Figure 14. The pulse shapes of a single channel and the combined beam are shown in Figure 15. Pulses with FWHM of ∼3 ns and repetition rate of 5 MHz have been obtained. The overall average/ peak power of the combined beam is 1.2/75.1 kW.

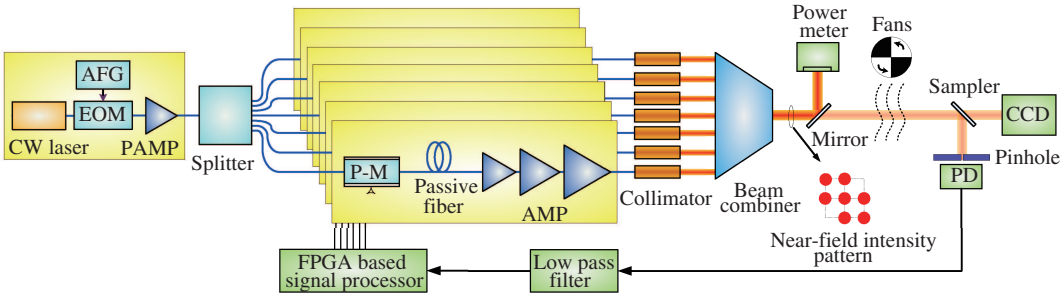

Figure 13 (Color online) Experimental setup of CBC of seven pulsed fiber lasers ©Copyright 2013 The Japan Society of Applied Physics. EOM: electro-optic modulator; AFG: arbitrary function generator; PAMP: pre-amplifier; P-M: phase modulator; AMP: amplifier; PD: photoelectric detector.

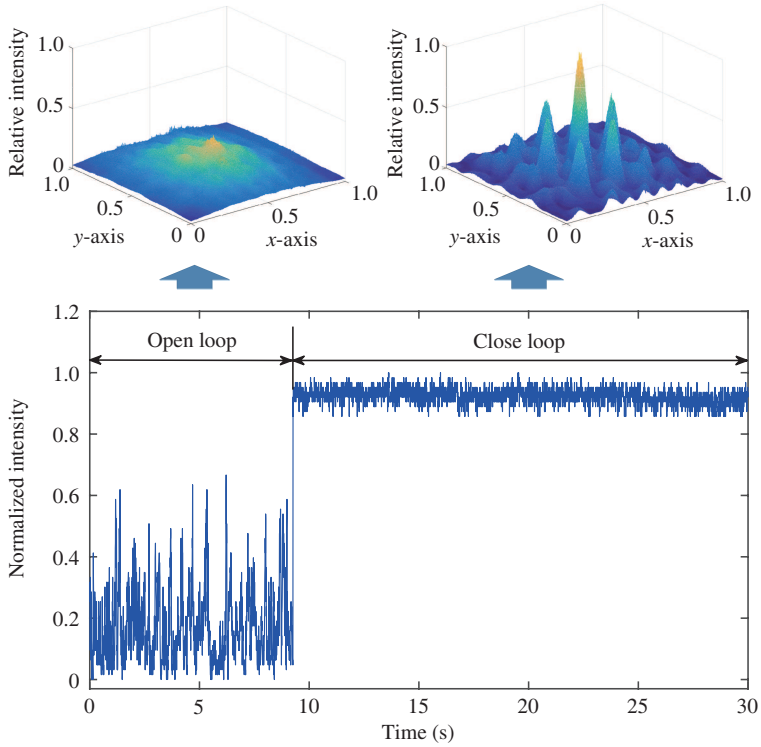

Figure 14 (Color online) Normalized intensity in the pinhole and long-exposure intensity pattern of the combined beam.

5.2 Coaxially aperture-filled CBC

In tiled CBC configuration, for fiber lasers emitted Gaussian-like fundamental modes, one physical limitation for brightness scaling is that the side-by-side interference will cause some combined power encircled in the side lobes. Coaxially aperture filled CBC could completely overcome the above deficiency in tiled CBC configurations. In this section, we mainly focus on our research results in this area and give some representative results achieved in the worldwide groups.

5.2.1 *CW coaxially aperture-filled CBC*

As one of a coaxially aperture filled CBC systems, the feasibility of CPBC technique for extending to multi-channel and high power has been investigated in our group in recent years. As similar in the general aperture filling structures, some imperfections will influence the combining efficiency of the CPBC system. These imperfections mainly include the intrinsic efficiency loss of the combining components, residual piston phase errors, beam size errors, path mismatch errors, polarization errors, intensity mismatch errors and high order wave-front errors. In theory, we have investigated the influences of mainly significant

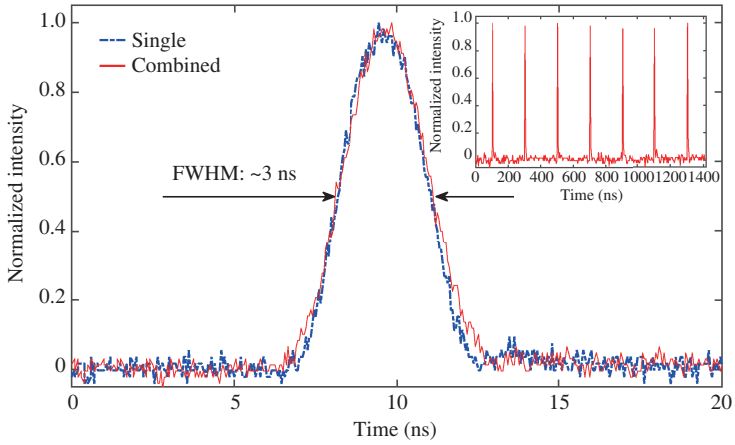

Figure 15 (Color online) Pulse shapes of a single channel and combined beam ©Copyright 2013 The Japan Society of Applied Physics.

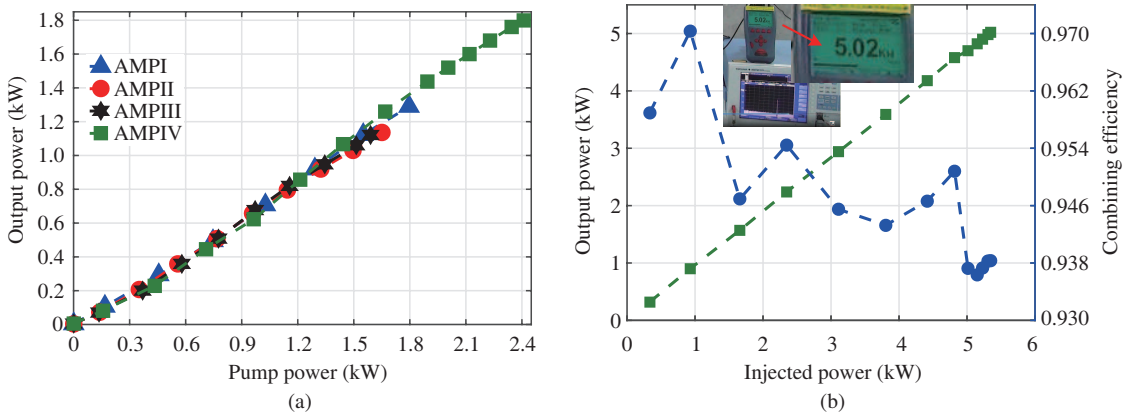

Figure 16 (Color online) Experimental results of the 5 kW CPBC system [273] ©Copyright 2017 Chinese Laser Press. (a) The relationship between the output laser power and the absorbed pump power of the four amplifiers; (b) combined output power and the combining efficiency as a function of the total injected power.

imperfections above-mentioned on CPBC system [267–269] and shown that CPBC has great potential for extending to multi-channel [23]. In experimental aspects, we demonstrated a 60 W four-channel CPBC system by using single frequency dithering technique in 2012 [270]. After that, we extended the CPBC technique to eight-channel by using a principle-concept low power system [252]. In 2013, we demonstrated a 481 W single frequency and linearly polarized system with near-diffraction-limited beam quality by coherent polarization locking [271]. In 2014, four 200 W level single frequency and PM fiber amplifiers were coaxially combined into a 680 W by CPBC technique with beam quality of M_x^2 ~1.24 and M_y^2 ~1.30 [272]. In 2016, along with our development on narrow linewidth and PM fiber amplifiers, CPBC of four 500-W-level fiber amplifiers and two kilowatt-level fiber amplifiers were demonstrated, which generates the first 2 kW CPBC system [23]. After that, by scaling the output power of single channel and optimizing the phase controller, defocus aberration compensation and high precision optical path control, the CPBC system has been broken through 5 kW power level with combining efficiency as high as 93.8% [273]. The relationship between the output laser power and the absorbed pump power of the four amplifiers is shown in Figure 16(a) and the combined output power and the combining efficiency as a function of the total injected power are shown in Figure 16(b). As shown in Figure 16(a), the output powers of the combined four channels are 1.29, 1.14, 1.12 and 1.8 kW, respectively. As shown in Figure 16(b), the combining efficiency of the CPBC system decreases within 3.2% along with the power scaling process.

As explicated in Subsection 4.3, except for CPBC technique, coaxially coherent beam combining could

Table 5 Typical research results on different coaxially coherent beam combining techniques

Year	Institution	Combining technique	Power (kW)	M^2	Combining efficiency	Ref.
2010	Lockheed Martin, USA	RIW	0.1	1.25	80%	[250]
2012	Soreq NRC, Israel	HPFC	3	1.17	–	[275]
2012	MIT Lincoln Lab, USA	DOE	1.93	1.1	79%	[276]
2014	Northrop Grumman, USA	DOE	2.4	1.2	80%	[217]
2016	AFRL, USA	DOE	5	1.06	82%	[248]
2017	NUDT, China	CPBC	2.16	1.2	94.5%	[23]
2017	MIT Lincoln Lab, USA	AFPL	1.27	–	–	[254]
2017	NUDT, China	CPBC	5.02	1.3	93.8%	[273]

also be fulfilled by diffractive optical element (DOE) [247, 248], re-imaging waveguide (RIW) [249, 250], high power fiber couplers (HPFC) [208, 253], spatial laser combiners (SLC) [274] and all-fiber-based photonic lantern (AFPL) [254]. The representative research results on different coaxially coherent beam combining techniques are listed in Table 5 [23, 217, 248, 250, 254, 273, 275, 276]. From Table 5, it could be seen that coaxially coherent beam combining based on DOE and CPBC has been beyond 5 kW output power with near-diffraction-limited beam qualities [248, 273]. Due to that the coaxially coherent beam combining techniques have strongly requirements on the synchronizations of phase distributions, polarizations, spatial mode distributions and time coherences among individual combined beam, so the combining efficiencies are susceptible to imperfections existed in the coherently combined systems. That is why the output power of coaxially coherent beam combining relatively developed slowly in the past years.

5.2.2 *Pulsed coaxially aperture-filled CBC*

Except for CW application, we also introduced CPBC technique into nanosecond, picosecond and femtosecond pulsed regimes in recent years. In pulsed CPBC system, some other imperfections, such as group velocity dispersion (GVD), and self-phase modulation (SPM), should also be carefully considered, especially in ultrafast femtosecond pulsed combining system. In theory, the influence of GVD and SPM on the combining efficiency of CPBC system was investigated and some mitigation strategies were proposed in our previous work [256]. In 2014, CPBC of a four-channel pulsed amplifier array in the picosecond regime was demonstrated [260], which generates a combined laser pulse with ∼480 ps pulse width at ∼60 MHz repetition rate with an average power of 88 W, excellent beam quality (M^2 ∼1.1) and combining efficiency of 90%. In 2016, CPBC of two-channel femtosecond pulsed combining system was conducted, which achieves 313 W output power with pulse width of 827 fs [277]. The time series with piston phase locking and system optimizing design are shown in Figure 17(a), which shows stable compensation effect of phase noise and optical path errors. Figure 17(b) shows the combining efficiency as a function of the combined power. As shown in Figure 17(b), along with power scaling, the combining efficiency of the CPBC system decreases from 87% to 79% before output power of 313 W while maintains well between output power of ∼110 and 313 W. Further power scaling the system, we found a sudden decrease of combining efficiency, which is induced by the beam quality deterioration of the individual beams. The autocorrelation traces of individual beam and the combined beam are shown in Figure 17(c). It is shown that high average power with 1.17 ps pulse width could be obtained with little pulse distortion compared with each single-channel pulse. Notably that 1 kW average power with 1 mJ pulse energy and 260 fs pulse duration and ∼700 W average power with 12 mJ pulse energy and 262 fs pulse duration had been achieved by CPBC technique [224, 278]. Quite recently, coherently beam combined beam with average output power of 1.8 kW, pulse energy of 4 mJ and pulse duration of 230 fs has been reported [279].

6 Future prospects and conclusion

Benefit from their unique properties, such as high brightness, high optical to optical conversion efficiency,

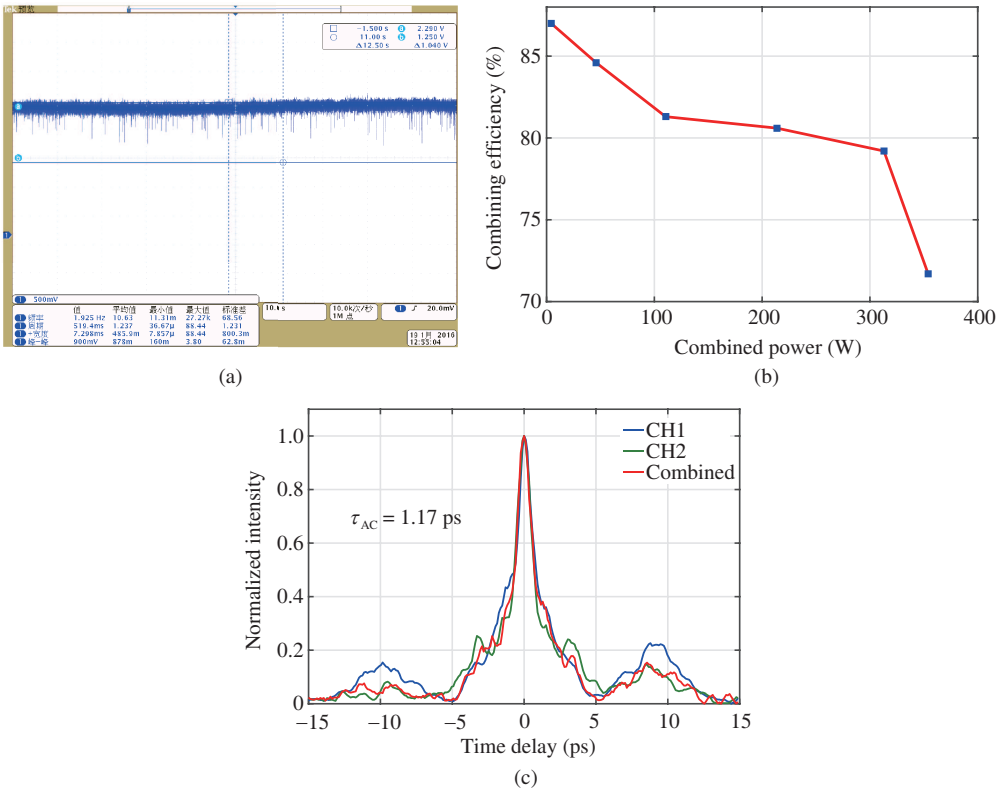

Figure 17 (Color online) Experimental results of the pulsed CPBC system [277] ©Copyright 2018 Astro Ltd. Reproduced by permission of IOP Publishing. (a) The time series with piston phase locking and system optimizing design; (b) the combining efficiency as a function of the combined power; (c) the autocorrelation traces of individual beam and the combined beam.

excellent beam quality, low cost of ownership, convenient thermal management and easy to maintenance, high power fiber lasers have been becoming one of the significant branches of laser technology and developed quickly during the past decade.

In this paper, we mainly review the development of high-power fiber lasers and their coherent beam combining in the recent decade by focusing on the relevant researches in our group. High-brightness pump sources, high-power-handling passive components, physical principles and efficient techniques for SBS, SRS, and TMI management are firstly retrospect. Then, high power fiber lasers with different spectral characteristics are reviewed, including narrow-linewidth, broadband and mid-infrared fiber lasers. Further, the key techniques and representative results for CBC in CW and pulsed regimes are demonstrated. Following their remarkable progresses, future prospects of fiber lasers and coherent beam combining technique are discussed below.

For high power broadband fiber lasers, SRS and TMI will determine their ultimate brightness extracting ability [280]. Despite that the predicted power limits in cladding-pumped fiber lasers are 27.8 and 52.5 kW by respectively using diode pumping and tandem pumping [280], restricted by manufacturing techniques of active fiber and passive fiber components, there is still a long distance to perform for reaching or beyond the power limits in the future. Even that the SRS and TMI suppressions could be simultaneously balanced by optimizing the injected seed characteristics, the pumping manners and the entire fiber system design, future innovations in fiber-suitable materials and new types of fiber designs are strongly expected to remarkably pushing the development of high power fiber lasers.

For high power narrow linewidth fiber lasers, along with power scaling, SRS, TMI and SBS will coexist and may be mutual-coupled, so future work need to investigate and optimize the system by comprehensively considering the above multiple detrimental issues. Further, aimed to more efficient employing in CBC system by alleviating the complex optical path errors control, linewidth narrowing

has been a new significant development trend and challenge for high power narrow linewidth fiber lasers. Besides, the intensity and frequency noise suppressions in high power narrow linwidth fiber lasers will be a new hotspot avenue for great potential applications in next-generation gravitational wave detection and some special frontier science [281].

For high power fiber lasers at 2 μm, further work could be focused on the pump brightness scaling, heat load management, and increase power handling capacity of fiber devices. Tandem pumping seems to be a promising technique to breakthrough these bottlenecks. With tandem pumping technique, the most efficient pumping method, i.e., resonant pumping, has an opportunity to become the reality at such long wavelength.

For CBC technique, future work could be aimed to large channels and higher output power without at the cost of losing combining efficiency and beam quality. In this case, at least two challenges should be broken through. The first one is to maintain control bandwidth of the phase controller with the increase of combined channels. As for this point, some new methods, such as CDMA-based single-frequency dithering technique [232], cascaded phase control [233, 234], extremum-seeking [282] and machine learning [283] could be incorporated into high power, large-channel coherent beam combining system to tentatively overcome this challenge. The second point is to prevent combining efficiency loss and/or beam quality degradation in high power, large-channel CBC system. This challenge could be overcome from three aspects: (i) The suppressing of higher order modes, linewidth broadening and polarization degradation in high power narrow linewidth fiber amplifiers; (ii) The whole optimizing of the control accuracies and ranges of piston, tilt, defocus errors controller; Multi-parameter integrated and compatible controlling and decoupling will be the crucial trend in the next; (iii) Efficient aperture filling in high power, large-channel CBC system. For tiled aperture beam combining, despite the combinable channels is easy to extend, a portion of power would be inevitably encircled into the side-lobes in the far field pattern and the beam quality and combining efficiency will be degraded. For coaxially aperture-filled CBC, the combined channels reported are obvious less than in tiled aperture beam combining systems. Optimizing designs or pioneering new coaxial aperture-filling techniques that are suitable for tens of channels with high combining efficiency are strongly required in the future.

Acknowledgements This work was supported by National Natural Science Foundation of China (Grant Nos. 61705264, 61705265). Authors would like to acknowledge Jinyong LENG, Hu XIAO, Yanxing MA, Jiangming XU, Xiaolin WANG, Zilun CHEN, Liangjin HUANG, Wei LIU, Tianyue HOU, Baolai YANG, and Zhaokai LOU in College of Advanced Interdisciplinary Studies, National University of Defense Technology for their collaboration.

References

1 Snitzer E. Proposed fiber cavities for optical masers. J Appl Phys, 1961, 32: 36–39
2 Richardson D J, Nilsson J, Clarkson W A. High power fiber lasers: current status and future perspectives. J Opt Soc Am B, 2010, 27: 63–92
3 Dong L, Samson B. Fiber Lasers: Basics, Technology, and Applications. Boca Raton: CRC Press, 2016
4 Zervas M N, Codemard C A. High power fiber lasers: a review. IEEE J Sel Top Quantum Electron, 2014, 20: 219–241
5 Liu Z, Zhou P, Xu X, et al. Coherent Beam Combining of High Average Power Fiber Lasers. Beijing: National Defense Industry Press, 2016
6 Stiles E. New developments in IPG fiber laser technology. In: Proceedings of the 5th International Workshop on Fiber Lasers, 2009
7 Shi W, Fang Q, Zhu X, et al. Fiber lasers and their applications [Invited]. Appl Opt, 2014, 53: 6554–6568
8 Huang L, Xu J, Ye J, et al. Power scaling of linearly polarized random fiber laser. IEEE J Sel Top Quantum Electron, 2018, 24: 1–8
9 Shi W, Schulzgen A, Amezcua R, et al. Fiber lasers and their applications: introduction. J Opt Soc Am B, 2017, 34: A1
10 Zhou J, Wang P, Zhou P. High power fiber laser technology: introduction. Chin J Laser, 2017, 44: 201000
11 Dawson J W, Messerly M J, Beach R J, et al. Analysis of the scalability of diffraction-limited fiber lasers and amplifiers to high average power. Opt Express, 2008, 16: 13240–13266
12 Zhu J, Zhou P, Ma Y, et al. Power scaling analysis of tandem-pumped Yb-doped fiber lasers and amplifiers. Opt Express, 2011, 19: 18645–18654
13 Ke W W, Wang X J, Bao X F, et al. Thermally induced mode distortion and its limit to power scaling of fiber lasers. Opt Express, 2013, 21: 14272–14281

14 Otto H J, Jauregui C, Limpert J, et al. Average power limit of Ytterbium-doped fiber-laser systems with nearly diffraction-limited beam quality. In: Proceedings of SPIE, San Francisco, 2015. 97280E
15 Zervas M N. Power scaling limits in high power fiber amplifiers due to transverse mode instability, thermal lensing, and fiber mechanical reliability. In: Proceedings of SPIE, San Francisco, 2018. 1051205
16 Shcherbakov E, Fomin V, Abramov A, et al. Industrial grade 100 kW power CW fiber laser. In: Advanced Solid State Lasers. Washington: Optical Society of America, 2013. ATh4A.2
17 Fan T Y. Laser beam combining for high-power, high-radiance sources. IEEE J Sel Top Quantum Electron, 2005, 11: 567–577
18 Brignon A. Coherent Laser Beam Combining. Weinheim: John Wiley & Sons, 2013
19 Liu Z J, Zhou P, Xu X J, et al. Coherent beam combining of high power fiber lasers: progress and prospect. Sci China Technol Sci, 2013, 56: 1597–1606
20 Honea E, Afzal R S, Savage-Leuchs M, et al. Advances in fiber laser spectral beam combining for power scaling. In: Proceedings of SPIE, San Francisco, 2016. 97300Y
21 Ma Y, Wang X, Zhou P, et al. Coherent beam combination of 137 W fiber amplifier array using single frequency dithering technique. Opt Lasers Eng, 2011, 49: 1089–1092
22 Su R, Zhou P, Wang X, et al. Active coherent beam combining of a five-element, 800 W nanosecond fiber amplifier array. Opt Lett, 2012, 37: 3978–3980
23 Liu Z, Ma P, Su R, et al. High-power coherent beam polarization combination of fiber lasers: progress and prospect. J Opt Soc Am B, 2017, 34: A7
24 Zhou P, Wang X, Ma Y, et al. Active and passive coherent beam combining of thulium-doped fiber lasers. In: Proceedings of SPIE, San Francisco, 2010. 784307
25 Ma P, Tao R, Su R, et al. 189 kW all-fiberized and polarization-maintained amplifiers with narrow linewidth and near-diffraction-limited beam quality. Opt Express, 2016, 24: 4187–4195
26 Yu H, Wang X, Zhang H, et al. Linearly-polarized fiber-integrated nonlinear CPA system for high-average-power femtosecond pulses generation at 1.06 μm. J Lightwave Technol, 2016, 34: 4271–4277
27 Jin X, Wang X, Zhou P, et al. Powerful 2 μm silica fiber sources: a review of recent progress and prospects. J Electron Sci Tech, 2015, 13: 315–327
28 Huang L, Wu H, Li R, et al. 414 W near-diffraction-limited all-fiberized single-frequency polarization-maintained fiber amplifier. Opt Lett, 2017, 42: 1–4
29 Du X, Zhang H, Xiao H, et al. High-power random distributed feedback fiber laser: from science to application. Annalen Der Physik, 2016, 528: 649–662
30 Xu J, Zhou P, Liu W, et al. Exploration in performance scaling and new application avenues of superfluorescent fiber source. IEEE J Sel Top Quantum Electron, 2018, 24: 1–10
31 Xiao H, Zhou P, Wang X, et al. Experimental investigation on 1018-nm high-power ytterbium-doped fiber amplifier. IEEE Photon Technol Lett, 2012, 24: 1088–1090
32 Xiao H, Zhou P, Wang X L, et al. High power 1018 nm ytterbium doped fiber laser with an output power of 309 W. Laser Phys Lett, 2013, 10: 065102
33 Xiao H, Leng J, Zhang H, et al. High-power 1018 nm ytterbium-doped fiber laser and its application in tandem pump. Appl Opt, 2015, 54: 8166
34 Yan P, Wang X, Li D, et al. High-power 1018 nm ytterbium-doped fiber laser with output of 805 W. Opt Lett, 2017, 42: 1193
35 Glick Y, Sintov Y, Zuitlin R, et al. Single-mode 230 W output power 1018 nm fiber laser and ASE competition suppression. J Opt Soc Am B, 2016, 33: 1392–1398
36 Yang H, Zhao W, Si J, et al. 126 W fiber laser at 1018 nm and its application in tandem pumped fiber amplifier. J Opt, 2016, 18: 125801
37 Gu G, Liu Z, Kong F, et al. Highly efficient ytterbium-doped phosphosilicate fiber lasers operating below 1020 nm. Opt Express, 2015, 23: 17693
38 Seah C P, Ng T Y, Chua S. 400 W Ytterbium-doped fiber oscillator at 1018nm. In: Advanced Solid State Lasers. Washington: Optical Society of America, 2015. ATu2A.33
39 Chen X, Wang J, Zhao X, et al. 307 W high-power 1018 nm monolithic tandem pump fiber source with effective thermal management. Chin Opt Lett, 2017, 15: 071407
40 Zhang H, Xiao H, Zhou P, et al. A high-power all-fiberized Yb-doped laser directly pumped by a laser diode emitting at long wavelength. Laser Phys Lett, 2013, 10: 095106
41 Huang L, Zhang H, Wang X, et al. Diode-pumped 1178-nm high-power Yb-doped fiber laser operating at 125 C. IEEE Photonic J, 2016, 8: 1–7
42 Kurkov A S. Oscillation spectral range of Yb-doped fiber lasers. Laser Phys Lett, 2007, 4: 93–102
43 Zhou P, Wang X, Xiao H, et al. Review on recent progress on Yb-doped fiber laser in a variety of oscillation spectral ranges. Laser Phys, 2012, 22: 823–831
44 Pask H M, Carman R J, Hanna D C, et al. Ytterbium-doped silica fiber lasers: versatile sources for the 1-1.2 μm region. IEEE J Sel Top Quantum Electron, 1995, 1: 2–13
45 Zhang H W, Xiao H, Zhou P, et al. 119-W monolithic single-mode 1173-nm Raman fiber laser. IEEE Photonic J, 2013, 5: 1501706
46 Zhang H, Zhou P, Xiao H, et al. Efficient Raman fiber laser based on random Rayleigh distributed feedback with record high power. Laser Phys Lett, 2014, 11: 075104

47 Du X, Zhang H, Wang X, et al. Short cavity-length random fiber laser with record power and ultrahigh efficiency. Opt Lett, 2016, 41: 571–574
48 Xiao H, Zhang H, Xu J, et al. 120 W monolithic Yb-doped fiber oscillator at 1150 nm. J Opt Soc Am B, 2017, 34: A63
49 Zhang H, Zhou P, Wang X, et al. Hundred-watt-level high power random distributed feedback Raman fiber laser at 1150 nm and its application in mid-infrared laser generation. Opt Express, 2015, 23: 17138–17144
50 Jin X, Lou Z, Chen Y, et al. High-power dual-wavelength Ho-doped fiber laser at >2 μm tandem pumped by a 1.15 μm fiber laser. Sci Rep, 2017, 7: 42402
51 Chen Y, Xiao H, Xu J, et al. Laser diode-pumped dual-cavity high-power fiber laser emitting at 1150 nm employing hybrid gain. Appl Opt, 2016, 55: 3824–3828
52 Wang J, Li C, Yan D. High power composite cavity fiber laser oscillator at 1120 nm. Opt Commun, 2017, 405: 318–322
53 Gu Y, Lei C, Liu J, et al. Side-pumping combiner for high-power fiber laser based on tandem pumping. Opt Eng, 2017, 56: 1
54 Xiao Q, Yan P, Ren H, et al. A side-pump coupler with refractive index valley configuration for fiber lasers and amplifiers. J Lightwave Technol, 2013, 31: 2715–2722
55 Lei C, Chen Z, Leng J, et al. The influence of fused depth on the side-pumping combiner for all-fiber lasers and amplifiers. J Lightwave Technol, 2017, 35: 1922–1928
56 Guo W, Chen Z, Li J, et al. A system for splicing double cladding fiber and glass cone and its splicing method. China Patent, CN103217741A, 2014-09-17
57 Zhou X F, Chen Z L, Hou J, et al. High power fiber end-cap with 6 kW output power. High Power Laser Part Beams, 2015, 27: 27120101
58 Lei C, Gu Y, Chen Z, et al. Incoherent beam combining of fiber lasers by an all-fiber 7 × 1 signal combiner at a power level of 14 kW. Opt Express, 2018, 26: 10421–10427
59 Zhou X, Chen Z, Wang Z, et al. Monolithic fiber end cap collimator for high-power free-space fiber-fiber coupling. Appl Opt, 2016, 55: 4001–4004
60 Zhi D, Ma Y, Chen Z, et al. Large deflection angle, high-power adaptive fiber optics collimator with preserved near-diffraction-limited beam quality. Opt Lett, 2016, 41: 2217–2220
61 Zhi D, Zhang Z, Ma Y, et al. Realization of large energy proportion in the central lobe by coherent beam combination based on conformal projection system. Sci Rep, 2017, 7: 2199
62 Guo W, Chen Z, Zhou H, et al. Cascaded cladding light extracting strippers for high power fiber lasers and amplifiers. IEEE Photonic J, 2014, 6: 1–6
63 Zhou H, Chen Z, Zhou X, et al. All-fiber 7×1 signal combiner with high beam quality for high-power fiber lasers. Chin Opt Lett, 2015, 13: 061406–61409
64 Li R, Xiao H, Leng J, et al. 2240 W high-brightness 1018 nm fiber laser for tandem pump application. Laser Phys Lett, 2017, 14: 125102
65 Gu Y, Leng J, Xiao H, et al. 5 kW all-fiber 1018 nm laser combining. High Power Laser Part Beams, 2017, 29: 29120101
66 Agrawal G. Nonlinear Fiber Optics. Manhattan: Academic Press, 2012
67 Lü H, Zhou P, Wang X, et al. Dynamics of stimulated Brillouin scattering in optical fibers without external feedback induced by frequency detuning from resonance. Opt Express, 2015, 23: 18117–18132
68 Lu H, Zhou P, Wang X, et al. Theoretical and numerical study of the threshold of stimulated brillouin scattering in multimode fibers. J Lightwave Technol, 2015, 33: 4464–4470
69 Leng J Y, Wang X L, Xiao H, et al. Suppressing the stimulated Brillouin scattering in high power fiber amplifiers by dual-single-frequency amplification. Laser Phys Lett, 2012, 9: 532–536
70 Huang L, Li L, Ma P, et al. 434 W all-fiber linear-polarization dual-frequency Yb-doped fiber laser carrying low-noise radio frequency signal. Opt Express, 2016, 24: 26722–26731
71 Ma P, Zhou P, Ma Y, et al. Single-frequency 332 W, linearly polarized Yb-doped all-fiber amplifier with near diffraction-limited beam quality. Appl Opt, 2013, 52: 4854
72 Huang L, Zhou Z C, Shi C, et al. Towards tapered-fiber-based all-fiberized high power narrow linewidth fiber laser. Sci China Technol Sci, 2018, 61: 971–981
73 Su R, Tao R, Wang X, et al. 2.43 kW narrow linewidth linearly polarized all-fiber amplifier based on mode instability suppression. Laser Phys Lett, 2017, 14: 085102
74 Smith R G. Optical power handling capacity of low loss optical fibers as determined by stimulated Raman and Brillouin scattering. Appl Opt, 1972, 11: 2489
75 Wang Y, Xu C Q, Po H. Analysis of Raman and thermal effects in kilowatt fiber lasers. Opt Commun, 2004, 242: 487–502
76 Jauregui C, Limpert J, Tünnermann A. Derivation of Raman treshold formulas for CW double-clad fiber amplifiers. Opt Express, 2009, 17: 8476–8490
77 Liu W, Ma P, Lv H, et al. General analysis of SRS-limited high-power fiber lasers and design strategy. Opt Express, 2016, 24: 26715–26721
78 Liu W, Ma P, Lv H, et al. Investigation of stimulated Raman scattering effect in high-power fiber amplifiers seeded by narrow-band filtered superfluorescent source. Opt Express, 2016, 24: 8708–8717
79 Liu W, Ma P, Miao Y, et al. Intrinsic mechanism for spectral evolution in single-frequency raman fiber amplifier.

IEEE J Sel Top Quantum Electron, 2018, 24: 1–8
80 Zhang L, Jiang H, Cui S, et al. Integrated ytterbium-Raman fiber amplifier. Opt Lett, 2014, 39: 1933–1936
81 Zhang H, Xiao H, Zhou P, et al. High power Yb-Raman combined nonlinear fiber amplifier. Opt Express, 2014, 22: 10248–10255
82 Zhang H, Tao R, Zhou P, et al. 1.5-kW Yb-Raman combined nonlinear fiber amplifier at 1120 nm. IEEE Photon Technol Lett, 2015, 27: 628–630
83 Xiao Q, Yan P, Li D, et al. Bidirectional pumped high power Raman fiber laser. Opt Express, 2016, 24: 6758–6768
84 Smith A V, Smith J J. Influence of pump and seed modulation on the mode instability thresholds of fiber amplifiers. Opt Express, 2012, 20: 24545–24558
85 Smith A V, Smith J J. Mode instability in high power fiber amplifiers. Opt Express, 2011, 19: 10180–10192
86 Eidam T, Wirth C, Jauregui C, et al. Experimental observations of the threshold-like onset of mode instabilities in high power fiber amplifiers. Opt Express, 2011, 19: 13218–13224
87 Jauregui C, Eidam T, Otto H J, et al. Physical origin of mode instabilities in high-power fiber laser systems. Opt Express, 2012, 20: 12912–12925
88 Ward B, Robin C, Dajani I. Origin of thermal modal instabilities in large mode area fiber amplifiers. Opt Express, 2012, 20: 11407–11422
89 Hu I, Zhu C, Zhang C, et al. Analytical time-dependent theory of thermally induced modal instabilities in high power fiber amplifiers. In: Proceedings of SPIE, San Francisco, 2013. 860109
90 Hansen K R, Alkeskjold T T, Broeng J, et al. Theoretical analysis of mode instability in high-power fiber amplifiers. Opt Express, 2013, 21: 1944
91 Tao R M, Ma P F, Wang X L, et al. Study of wavelength dependence of mode instability based on a semi-analytical model. IEEE J Quantum Electron, 2015, 51: 1–6
92 Tao R, Ma P, Wang X, et al. Influence of core NA on thermal-induced mode instabilities in high power fiber amplifiers. Laser Phys Lett, 2015, 12: 085101
93 Tao R, Wang X, Zhou P. Comprehensive theoretical study of mode instability in high-power fiber lasers by employing a universal model and its implications. IEEE J Sel Top Quantum Electron, 2018, 24: 1–19
94 Tao R, Ma P, Wang X, et al. 13 kW monolithic linearly polarized single-mode master oscillator power amplifier and strategies for mitigating mode instabilities. Photon Res, 2015, 3: 86–93
95 Tao R, Ma P, Wang X, et al. Mitigating of modal instabilities in linearly-polarized fiber amplifiers by shifting pump wavelength. J Opt, 2015, 17: 045504
96 Dajani I, Flores A, Holten R, et al. Multi-kilowatt power scaling and coherent beam combining of narrow-linewidth fiber lasers. In: Proceedings of SPIE, San Francisco, 2016. 972801
97 Wirth C, Schmidt O, Tsybin I, et al. High average power spectral beam combining of four fiber amplifiers to 8.2 kW. Opt Lett, 2011, 36: 3118–3120
98 Zheng Y, Yang Y, Wang J, et al. 108 kW spectral beam combination of eight all-fiber superfluorescent sources and their dispersion compensation. Opt Express, 2016, 24: 12063–12071
99 Karow M, Basu C, Kracht D, et al. TEM 00 mode content of a two stage single-frequency Yb-doped PCF MOPA with 246 W of output power. Opt Express, 2012, 20: 5319–5324
100 Gapontsev V, Avdokhin A, Kadwani P, et al. SM green fiber laser operating in CW and QCW regimes and producing over 550 W of average output power. In: Proceedings of SPIE, San Francisco, 2014. 896407
101 Zhou P, Huang L, Xu J M, et al. High power linearly polarized fiber laser: generation, manipulation and application. Sci China Technol Sci, 2017, 60: 1784–1800
102 Ruffin A B, Li M J, Chen X, et al. Brillouin gain analysis for fibers with different refractive indices. Opt Lett, 2005, 30: 3123–3125
103 Brar K, Savage-Leuchs M, Henrie J, et al. Threshold power and fiber degradation induced modal instabilities in high-power fiber amplifiers based on large mode area fibers. In: Proceedings of SPIE, San Francisco, 2014. 89611R
104 Xiao H, Dong X L, Zhou P, et al. A 168-W high-power single-frequency amplifier in an all-fiber configuration. Chin Phys B, 2012, 21: 034207
105 Wang X L, Zhou P, Xiao H, et al. 310 W single-frequency all-fiber laser in master oscillator power amplification configuration 310 W single-frequency all-fiber laser. Laser Phys Lett, 2012, 9: 591–595
106 Robin C, Dajani I, Pulford B. Modal instability-suppressing, single-frequency photonic crystal fiber amplifier with 811 W output power. Opt Lett, 2014, 39: 666–669
107 Jeong Y, Nilsson J, Sahu J K, et al. Single-frequency, single-mode, plane-polarized ytterbium-doped fiber master oscillator power amplifier source with 264 W of output power. Opt Lett, 2005, 30: 459–461
108 Hildebrandt M, Frede M, Kwee P, et al. Single-frequency master-oscillator photonic crystal fiber amplifier with 148 W output power. Opt Express, 2006, 14: 11071–11076
109 Gray S, Liu A, Walton D T, et al. 502 Watt, single transverse mode, narrow linewidth, bidirectionally pumped Yb-doped fiber amplifier. Opt Express, 2007, 15: 17044–17050
110 Jeong Y, Nilsson J, Sahu J K, et al. Power scaling of single-frequency ytterbium-doped fiber master-oscillator power-amplifier sources up to 500 W. IEEE J Sel Top Quantum Electron, 2007, 13: 546–551
111 Mermelstein M D, Yablon A D, Headley C, et al. All-fiber 194 W single-frequency single-mode Yb-doped master-oscillator power-amplifier. In: Proceedings of SPIE, San Francisco, 2008. 68730L
112 Dajani I, Vergien C, Robin C, et al. Experimental and theoretical investigations of photonic crystal fiber amplifier with 260 W output. Opt Express, 2009, 17: 24317–24333

113 Zeringue C, Vergien C, Dajani I. Pump-limited, 203 W, single-frequency monolithic fiber amplifier based on laser gain competition. Opt Lett, 2011, 36: 618–620

114 Zhu C, Hu I, Ma X, et al. Single-frequency and single-transverse mode Yb-doped CCC fiber MOPA with robust polarization SBS-free 511W output. In: Advances in Optical Materials. Washington: Optical Society of America, 2011. AMC5

115 Theeg T, Sayinc H, Neumann J, et al. All-fiber counter-propagation pumped single frequency amplifier stage with 300-W output power. IEEE Photon Technol Lett, 2012, 24: 1864–1867

116 Zhang L, Cui S, Liu C, et al. 170 W, single-frequency, single-mode, linearly-polarized, Yb-doped all-fiber amplifier. Opt Express, 2013, 21: 5456–5462

117 Theeg T, Ottenhues C, Sayinc H, et al. Core-pumped single-frequency fiber amplifier with an output power of 158 W. Opt Lett, 2016, 41: 9–12

118 Wang X, Zhou P, Xiao H, et al. Narrow linewidth all-fiber laser with 666 W power output. High Power Laser Particle Beams, 2012, 24: 1261–1262

119 Ran Y, Tao R, Ma P, et al. 560 W all fiber and polarization-maintaining amplifier with narrow linewidth and near-diffraction-limited beam quality. Appl Opt, 2015, 54: 7258–7263

120 Beier F, Hupel C, Kuhn S, et al. Single mode 43 kW output power from a diode-pumped Yb-doped fiber amplifier. Opt Express, 2017, 25: 14892–14899

121 Li T, Zha C, Sun Y, et al. 3.5 kW bidirectionally pumped narrow-linewidth fiber amplifier seeded by white-noise-source phase-modulated laser. Laser Phys, 2018, 28: 105101

122 Yu C X, Shatrovoy O, Fan T Y, et al. Diode-pumped narrow linewidth multi-kilowatt metalized Yb fiber amplifier. Opt Lett, 2016, 41: 5202–5205

123 Platonov N, Yagodkin R, De La Cruz J, et al. Up to 2.5-kW on non-PM fiber and 2.0-kW linear polarized on PM fiber narrow linewidth CW diffraction-limited fiber amplifiers in all-fiber format. In: Proceedings of SPIE, San Francisco, 2018. 105120E

124 Edgecumbe J, Bjrk D, Galipeau J, et al. Kilowatt-level PM amplifiers for beam combining. In: Frontiers in Optics. Washington: Optical Society of America, 2008. FTuJ2

125 Goodno G D, McNaught S J, Rothenberg J E, et al. Active phase and polarization locking of a 14 kW fiber amplifier. Opt Lett, 2010, 35: 1542–1544

126 Guintrand C, Edgecumbe J, Farley K, et al. Stimulated Brillouin scattering threshold variations due to bend-induced birefringence in a non-polarization-maintaining fiber amplifier. In: Laser and Electro-Optics. Washington: Optical Society of America, 2014. JW2A.23

127 Flores A, Robin C, Lanari A, et al. Pseudo-random binary sequence phase modulation for narrow linewidth, kilowatt, monolithic fiber amplifiers. Opt Express, 2014, 22: 17735–17744

128 Yagodkin R, Platonov N, Yusim A, et al. $>$ 1.5 kW narrow linewidth CW diffraction-limited fiber amplifier with 40nm bandwidth. In: Proceedings of SPIE, San Francisco, 2015. 972807

129 Xu Y, Fang Q, Qin Y, et al. 2 kW narrow spectral width monolithic continuous wave in a near-diffraction-limited fiber laser. Appl Opt, 2015, 54: 9419–9421

130 Nold J, Strecker M, Liem A, et al. Narrow linewidth single mode fiber amplifier with 2.3 kW average power. In: Lasers and Electro-Optics. Washington: Optical Society of America, 2015. CJ_11_4

131 Yu C X, Shatrovoy O, Fan T Y. All-glass fiber amplifier pumped by ultrahigh brightness pump. In: Proceedings of SPIE, San Francisco, 2015. 972806

132 Avdokhin A, Gapontsev V, Kadwani P, et al. High average power quasi-CW single-mode green and UV fiber lasers. In: Proceedings of SPIE, San Francisco, 2015. 934704

133 Beier F, Hupel C, Nold J, et al. Narrow linewidth, single mode 3 kW average power from a directly diode pumped ytterbium-doped low NA fiber amplifier. Opt Express, 2016, 24: 6011–6020

134 Naderi N A, Flores A, Anderson B M, et al. Beam combinable, kilowatt, all-fiber amplifier based on phase-modulated laser gain competition. Opt Lett, 2016, 41: 3964–3967

135 Kanskar M, Zhang J, Kaponen J, et al. Narrowband transverse-modal-instability (TMI)-free Yb-doped fiber amplifiers for directed energy applications. In: Proceedings of SPIE, San Francisco, 2018. 105120F

136 Yu H, Zhang H, lv H, et al. 315 kW direct diode-pumped near diffraction-limited all-fiber-integrated fiber laser. Appl Opt, 2015, 54: 4556–4560

137 Yu H, Wang X, Tao R, et al. 15 kW, near-diffraction-limited, high-efficiency, single-end-pumped all-fiber-integrated laser oscillator. Appl Opt, 2014, 53: 8055–8059

138 Yang B, Zhang H, Wang X, et al. Mitigating transverse mode instability in a single-end pumped all-fiber laser oscillator with a scaling power of up to 2 kW. J Opt, 2016, 18: 105803

139 Yang B, Zhang H, Shi C, et al. Mitigating transverse mode instability in all-fiber laser oscillator and scaling power up to 25 kW employing bidirectional-pump scheme. Opt Express, 2016, 24: 27828–27835

140 Yang B, Zhang H, Shi C, et al. 3.05 kW monolithic fiber laser oscillator with simultaneous optimizations of stimulated Raman scattering and transverse mode instability. J Opt, 2018, 20: 025802

141 Yang B, Zhang H, Ye Q, et al. 4.05 kW monolithic fiber laser oscillator based on home-made large mode area fiber Bragg gratings. Chin Opt Lett, 2018, 16: 031407

142 Huang L, Wang W, Leng J, et al. Experimental investigation on evolution of the beam quality in a 2-kW high power fiber amplifier. IEEE Photon Technol Lett, 2014, 26: 33–36

143 Xu J, Huang L, Leng J, et al. 101 kW superfluorescent source in all-fiberized MOPA configuration. Opt Express,

2015, 23: 5485–5490
144 Zhou P, Xiao H, Leng J, et al. High-power fiber lasers based on tandem pumping. J Opt Soc Am B, 2017, 34: A29
145 Zhang H, Yang B, Wang X, et al. Home-produced fiber Bragg gratings-based all-fiber oscillator with the output power exceeding 5.2 kW. Chin J Laser, 2018, 45: 0415002
146 Xu J M, Ye J, Zhou P, et al. Tandem pumping architecture enabled high power random fiber laser with near-diffraction-limited beam quality. Sci China Technol Sci, 2019, 62: 80–86
147 Ikoma S, Nguyen H K, Kashiwagi M, et al. 3 kW single stage all-fiber Yb-doped single-mode fiber laser for highly reflective and highly thermal conductive materials processing. In: Proceedings of SPIE, San Francisco, 2017. 100830Y
148 Shima K, Ikoma S, Uchiyama K, et al. 5-kW single stage all-fiber Yb-doped single-mode fiber laser for materials processing. In: Proceedings of SPIE, San Francisco, 2018. 105120C
149 Yang B, Shi C, Zhang H, et al. Monolithic fiber laser oscillator with record high power. Laser Phys Lett, 2018, 15: 075106
150 Xiao Y, Brunet F, Kanskar M, et al. 1-kilowatt CW all-fiber laser oscillator pumped with wavelength-beam-combined diode stacks. Opt Express, 2012, 20: 3296–3301
151 Yu H, Kliner D A V, Liao K, et al. 1.2-kW single-mode fiber laser based on 100-W high-brightness pump diodes. In: Proceedings of SPIE, San Francisco, 2012. 82370G
152 Ruppik S, Becker F, Grundmann F, et al. High-power disk and fiber lasers: a performance comparison. In: Proceedings of SPIE, San Francisco, 2012. 82350V
153 Khitrov V, Minelly J D, Tumminelli R, et al. 3kW single-mode direct diode-pumped fiber laser. In: Proceedings of SPIE, San Francisco, 2014. 89610V
154 Mashiko Y, Nguyen H K, Kashiwagi M, et al. 2 kW single-mode fiber laser with 20-m long delivery fiber and high SRS suppression. In: Proceedings of SPIE, San Francisco, 2016. 972805
155 Tanaka D. High power fibre lasers for industrial applications. In: Proceedings of Conference on Lasers and Electro-Optics Pacific Rim, 2017
156 Yao T, Ji J, Nilsson J. Ultra-low quantum-defect heating in ytterbium-doped aluminosilicate fibers. J Lightwave Technol, 2014, 32: 429–434
157 Liu Z, Zhao Y. Investigation on the nonlinear problem in high power fiber laser. In: Proceedings of LASER 2016, Beijing. 2016
158 Lin A, Zhan H, Peng K, et al. 10 kW-level pump-gain integrated functional laser fiber. High Power Laser Part Beams, 2018, 30: 60101
159 Lin H H, Tang X, Li C Y, et al. 10.6 kW high-brightness cascaded-end-pumped monolithic fiber lasers directly pumped by laser diodes (in Chinese). Chin J Laser, 2018, 45: 0315001
160 Shiner B. The impact of fiber laser technology on the world wide material processing market. In: Proceedings of CLEO: Applications and Technology 2013. Washington: Optical Society of America, 2013. AF2J.1
161 Wang J, Yan D, Xiong S, et al. High power all-fiber amplifier with different seed power injection. Opt Express, 2016, 24: 14463–14469
162 Zhan H, Liu Q, Wang Y, et al. 5 kW GTWave fiber amplifier directly pumped by commercial 976 nm laser diodes. Opt Express, 2016, 24: 27087–27095
163 Fang Q, Li J, Shi W, et al. 5 kW near-diffraction-limited and 8 kW high-brightness monolithic continuous wave fiber lasers directly pumped by laser diodes. IEEE Photonic J, 2017, 9: 1–7
164 Wang J, Yan D, Xiong S, et al. Mode instability in high power all-fiber amplifier with large-mode-area gain fiber. Opt Commun, 2017, 396: 123–126
165 Xiao Q, Li D, Huang Y, et al. Directly diode and bi-directional pumping 6 kW continuous-wave all-fibre laser. Laser Phys, 2018, 28: 125107
166 Jackson S D, Sabella A, Lancaster D G. Application and development of high-power and highly efficient silica-based fiber lasers operating at 2 μm. IEEE J Sel Top Quantum Electron, 2007, 13: 567–572
167 Geng J, Wang Q, Lee Y, et al. Development of eye-safe fiber lasers near 2 μm. IEEE J Sel Top Quant Electron, 2014, 20: 150–160
168 Koch G J, Beyon J Y, Barnes B W, et al. High-energy 2 μm Doppler lidar for wind measurements. Opt Eng, 2007, 46: 116201
169 Fried N M. Thulium fiber laser lithotripsy: an in vitro analysis of stone fragmentation using a modulated 110-watt Thulium fiber laser at 1.94 microm. Lasers Surg Med, 2005, 37: 53–58
170 Gesierich W, Reichenberger F, Fertl A, et al. Endobronchial therapy with a thulium fiber laser (1940 nm). J Thorac Cardiov Sur, 2014, 147: 1827–1832
171 Mingareev I, Weirauch F, Olowinsky A, et al. Welding of polymers using a 2 m thulium fiber laser. Opt Laser Tech, 2012, 44: 2095–2099
172 Scholle K, Schäfer M, Lamrini S, et al. All-fiber linearly polarized high power 2-μm single mode Tm-fiber laser for plastic processing and Ho-laser pumping applications. In: Proceedings of SPIE, San Francisco, 2018. 105120O
173 Simakov N, Davidson A, Hemming A, et al. Mid-infrared generation in ZnGeP2 pumped by a monolithic, power scalable 2-μm source. In: Proceedings of SPIE, San Francisco, 2012. 82373K
174 Leindecker N, Marandi A, Byer R L, et al. Octave-spanning ultrafast OPO with 2.6-6.1 μm instantaneous bandwidth pumped by femtosecond Tm-fiber laser. Opt Express, 2012, 20: 7046–7053
175 Kubat I, Petersen C R, Møller U V, et al. Thulium pumped mid-infrared 0.9-9 μm supercontinuum generation in concatenated fluoride and chalcogenide glass fibers. Opt Express, 2014, 22: 3959–3967

176 Petersen C R, Møller U V, Kubat I, et al. Mid-infrared supercontinuum covering the 1.4–13.3 μm molecular fingerprint region using ultra-high NA chalcogenide step-index fibre. Nat Photon, 2014, 8: 830–834

177 Goodno G D, Book L D, Rothenberg J E. Low-phase-noise, single-frequency, single-mode 608 W thulium fiber amplifier. Opt Lett, 2009, 34: 1204–1206

178 Moulton P F, Rines G A, Slobodtchikov E V, et al. Tm-doped fiber lasers: fundamentals and power scaling. IEEE J Sel Top Quantum Electron, 2009, 15: 85–92

179 Ehrenreich T, Leveille R, Majid I, et al. 1-kW, all-glass Tm: fiber laser. In: Proceedings of SPIE, San Francisco, 2010. 758016

180 Hemming A, Simakov N, Davidson A, et al. A monolithic cladding pumped holmium-doped fibre laser. In: Proceedings of CLEO: Science and Innovations. San Jose: Optical Society of America, 2013. CW1M.1

181 Walbaum T, Heinzig M, Schreiber T, et al. Monolithic thulium fiber laser with 567 W output power at 1970 nm. Opt Lett, 2016, 41: 2632

182 Newburgh G A, Zhang J, Dubinskii M. Tm-doped fiber laser resonantly diode-cladding-pumped at 1620 nm. Laser Phys Lett, 2017, 14: 125101

183 Moulton P F. High power Tm: silica fiber lasers: current status, prospects and challenges. In: Proceedings of Lasers and Electro-Optics Europe. San Jose: Optical Society of America, 2011. TF2_3

184 Creeden D, Johnson B R, Rines G A, et al. High power resonant pumping of Tm-doped fiber amplifiers in core- and cladding-pumped configurations. Opt Express, 2014, 22: 29067–29080

185 Meleshkevich M, Platonov N, Gapontsev D, et al. 415 W single-mode CW thulium fiber laser in all-fiber format. In: Proceedings of European Conference on Lasers and Electro-Optics. San Jose: Optical Society of America, 2007. CP2_3

186 Wang X, Zhou P, Zhang H, et al. 100 W-level Tm-doped fiber laser pumped by 1173 nm Raman fiber lasers. Opt Lett, 2014, 39: 4329–4332

187 Wang Y, Yang J, Huang C, et al. High power tandem-pumped thulium-doped fiber laser. Opt Express, 2015, 23: 2991–2998

188 Jin X, Lee E, Luo J, et al. High-efficiency ultrafast Tm-doped fiber amplifier based on resonant pumping. Opt Lett, 2018, 43: 1431–1434

189 Sincore A, Bradford J D, Cook J, et al. High average power thulium-doped silica fiber lasers: review of systems and concepts. IEEE J Sel Top Quantum Electron, 2018, 24: 1–8

190 Shardlow P C, Jain D, Parker R, et al. Optimising Tm-doped silica fibres for high lasing efficiency. In: Proceedings of the European Conference on Lasers and Electro-Optics. Washington: Optical Society of America, 2015. CJ_14_3

191 Tumminelli R, Petit V, Carter A, et al. Highly doped and highly efficient Tm doped fiber laser. In: Proceedings of SPIE, San Francisco, 2018. 105120M

192 Shardlow P C, Simakov N, Billaud A, et al. Holmium doped fibre optimised for resonant cladding pumping. In: Proceedings of Lasers and Electro-Optics. Washington: Optical Society of America, 2017. CJ_11_4

193 Wang X, Zhou P, Wang X, et al. 102 W monolithic single frequency Tm-doped fiber MOPA. Opt Express, 2013, 21: 32386–32392

194 Wang X, Jin X, Wu W, et al. 310-W single frequency Tm-Doped all-fiber MOPA. IEEE Photon Technol Lett, 2015, 27: 677–680

195 Wang X, Jin X, Zhou P, et al. All-fiber-integrated narrowband nanosecond pulsed Tm-doped fiber MOPA. IEEE Photon Technol Lett, 2015, 27: 1473–1476

196 Wang X, Jin X, Zhou P, et al. All-fiber high-average power nanosecond-pulsed master-oscillator power amplifier at 2 μm with mJ-level pulse energy. Appl Opt, 2016, 55: 1941–1945

197 Jin X, Wang X, Xu J, et al. High-power thulium-doped all-fibre amplified spontaneous emission sources. J Opt, 2015, 17: 045702

198 Jin X, Wang X, Xu J, et al. High-power thulium-doped all-fiber superfluorescent source with ultranarrow linewidth. IEEE Photonic J, 2015, 7: 1–6

199 Wang X, Jin X, Zhou P, et al. High power, widely tunable, narrowband superfluorescent source at 2 m based on a monolithic Tm-doped fiber amplifier. Opt Express, 2015, 23: 3382–3389

200 Wang X, Zhou P, Miao Y, et al. Raman fiber laser-pumped high-power, efficient Ho-doped fiber laser. J Opt Soc Am B, 2014, 31: 2476

201 Jin X, Du X, Wang X, et al. High-power ultralong-wavelength Tm-doped silica fiber laser cladding-pumped with a random distributed feedback fiber laser. Sci Rep, 2016, 6: 30052

202 Smith A V, Smith J J. Mode instability thresholds for Tm-doped fiber amplifiers pumped at 790 nm. Opt Express, 2016, 24: 975–992

203 Tao R, Zhou P, Xiao H, et al. Theoretical study of high power mode instabilities in 2 μm thulium-doped fiber amplifiers. In: Proceedings of the 16th International Conference on Laser Optics, St. Petersburg, 2014

204 Bochove E J, Shakir S A. Analysis of a spatial-filtering passive fiber laser beam combining system. IEEE J Sel Top Quantum Electron, 2009, 15: 320–327

205 Yang Y, Hu M, He B, et al. Passive coherent beam combining of four Yb-doped fiber amplifier chains with injection-locked seed source. Opt Lett, 2013, 38: 854–856

206 Huo Y, Cheo P K, King G G. Fundamental mode operation of a 19-core phase-locked Yb-doped fiber amplifier. Opt Express, 2004, 12: 6230–6239

207 Corcoran C J, Durville F. Experimental demonstration of a phase-locked laser array using a self-Fourier cavity. Appl

Phys Lett, 2005, 86: 201118
208 Wang B, Mies E, Minden M, et al. All-fiber 50 W coherently combined passive laser array. Opt Lett, 2009, 34: 863–865
209 Chen Z, Hou J, Zhou P, et al. Mutual injection-locking and coherent combining of two individual fiber lasers. IEEE J Quantum Electron, 2008, 44: 515–519
210 Steinhausser B, Brignon A, Lallier E, et al. High energy, single-mode, narrow-linewidth fiber laser source using stimulated Brillouin scattering beam cleanup. Opt Express, 2007, 15: 6464–6469
211 Kong H J, Yoon J W, Shin J S, et al. Long-term stabilized two-beam combination laser amplifier with stimulated Brillouin scattering mirrors. Appl Phys Lett, 2008, 92: 021120
212 Rothenberg J E. Passive coherent phasing of fiber laser arrays. In: Proceedings of SPIE, San Francisco, 2008. 687315
213 Yu C X, Augst S J, Redmond S M, et al. Coherent combining of a 4 kW, eight-element fiber amplifier array. Opt Lett, 2011, 36: 2686–2688
214 Wang X, Zhou P, Ma Y, et al. Active phasing a nine-element 1.14 kW all-fiber two-tone MOPA array using SPGD algorithm. Opt Lett, 2011, 36: 3121–3123
215 Wang X, Leng J, Zhou P, et al. 1.8-kW simultaneous spectral and coherent combining of three-tone nine-channel all-fiber amplifier array. Appl Phys B, 2012, 107: 785–790
216 Flores A, Ehrehreich T, Holten R, et al. Multi-kW coherent combining of fiber lasers seeded with pseudo random phase modulated light. In: Proceedings of SPIE, San Francisco, 2016. 97281Y
217 McNaught S J, Thielen P A, Adams L N, et al. Scalable coherent combining of kilowatt fiber amplifiers into a 2.4-kW beam. IEEE J Sel Top Quantum Electron, 2014, 20: 174–181
218 Yu C X, Kansky J E, Shaw S E J, et al. Coherent beam combining of large number of PM fibres in 2-D fibre array. Electron Lett, 2006, 42: 1024–1025
219 Huang Z, Tang X, Luo Y, et al. Active phase locking of thirty fiber channels using multilevel phase dithering method. Rev Sci Instrum, 2016, 87: 033109
220 Su R, Zhou P, Wang X, et al. Phase locking of a coherent array of 32 fiber lasers. High Power Laser Part Beams, 2014, 26: 10101
221 Bourderionnet J, Bellanger C, Primot J, et al. Collective coherent phase combining of 64 fibers. Opt Express, 2011, 19: 17053–17058
222 Bellanger C, Toulon B, Primot J, et al. Collective phase measurement of an array of fiber lasers by quadriwave lateral shearing interferometry for coherent beam combining. Opt Lett, 2010, 35: 3931–3933
223 Seise E, Klenke A, Limpert J, et al. Coherent addition of fiber-amplified ultrashort laser pulses. Opt Express, 2010, 18: 27827–27835
224 Müller M, Kienel M, Klenke A, et al. 1 kW 1 mJ eight-channel ultrafast fiber laser. Opt Lett, 2016, 41: 3439–3442
225 Goodno G D, Asman C P, Anderegg J, et al. Brightness-scaling potential of actively phase-locked solid-state laser arrays. IEEE J Sel Top Quantum Electron, 2007, 13: 460–472
226 Xiao R, Hou J, Liu M, et al. Coherent combining technology of master oscillator power amplifier fiber arrays. Opt Express, 2008, 16: 2015–2022
227 Vorontsov M A, Carhart G W, Ricklin J C. Adaptive phase-distortioncorrection based on parallel gradient-descent optimization. Opt Lett, 1997, 22: 907–909
228 Zhou P, Liu Z, Wang X, et al. Coherent beam combination of two-dimensional high power fiber amplifier array using stochastic parallel gradient descent algorithm. Appl Phys Lett, 2009, 94: 231106
229 Zhou P, Liu Z, Wang X, et al. Coherent beam combining of fiber amplifiers using stochastic parallel gradient descent algorithm and its application. IEEE J Sel Top Quantum Electron, 2009, 15: 248–256
230 Shay T M. Theory of electronically phased coherent beam combination without a reference beam. Opt Express, 2006, 14: 12188–12195
231 Ma Y, Zhou P, Wang X, et al. Coherent beam combination with single frequency dithering technique. Opt Lett, 2010, 35: 1308–1310
232 Jiang M, Su R, Zhang Z, et al. Coherent beam combining of fiber lasers using a CDMA-based single-frequency dithering technique. Appl Opt, 2017, 56: 4255–4260
233 Su R T, Zhou P, Wang X L, et al. High power narrow-linewidth nanosecond all-fiber lasers and their actively coherent beam combination. IEEE J Sel Top Quantum Electron, 2014, 20: 206–218
234 Su R, Zhang Z, Zhou P, et al. Coherent beam combining of a fiber lasers array based on cascaded phase control. IEEE Photon Technol Lett, 2016, 28: 2585–2588
235 Taylor J R, Anderson M S, Bunton P H. High-speed tilt mirror for image stabilization. Appl Opt, 1999, 38: 219–223
236 Wilcox C C, Andrews J R, Restaino S R, et al. Analysis of a combined tip-tilt and deformable mirror. Opt Lett, 2006, 31: 679–681
237 Wang X, Wang X, Zhou P, et al. 350-W coherent beam combining of fiber amplifiers with tilt-tip and phase-locking control. IEEE Photon Technol Lett, 2012, 24: 1781–1784
238 Vorontsov M A, Weyrauch T, Beresnev L A, et al. Adaptive array of phase-locked fiber collimators: analysis and experimental demonstration. IEEE J Sel Top Quantum Electron, 2009, 15: 269–280
239 Geng C, Luo W, Tan Y, et al. Experimental demonstration of using divergence cost-function in SPGD algorithm for coherent beam combining with tip/tilt control. Opt Express, 2013, 21: 25045–25055
240 Geng C, Li X, Zhang X, et al. Coherent beam combination of an optical array using adaptive fiber optics collimators. Opt Commun, 2011, 284: 5531–5536

241 Zhi D, Ma P, Ma Y, et al. Novel adaptive fiber-optics collimator for coherent beam combination. Opt Express, 2014, 22: 31520–31528
242 Zhi D, Ma Y, Ma P, et al. Adaptive fiber optics collimator based on flexible hinges. Appl Opt, 2014, 53: 5434–5438
243 Beresnev L A, Weyrauch T, Vorontsov M A, et al. Development of adaptive fiber collimators for conformal fiber-based beam projection systems. In: Proceedings of SPIE, San Francisco, 2008. 709008
244 Anderegg J, Brosnan S, Cheung E, et al. Coherently coupled high-power fiber arrays. In: Proceedings of SPIE, San Francisco, 2006. 61020U
245 Fan X, Liu J, Liu J, et al. Coherent combining of a seven-element hexagonal fiber array. Opt Laser Tech, 2010, 42: 274–279
246 Liu Z, Xu X, Chen J, et al. Multi-beam high-duty-cycle combiner. 2009, CN200920065407
247 Cheung E C, Ho J G, Goodno G D, et al. Diffractive-optics-based beam combination of a phase-locked fiber laser array. Opt Lett, 2008, 33: 354–356
248 Flores A, Dajani I. Kilowatt-class, all-fiber amplifiers for beam combining. In: Proceedings of SPIE, 2016
249 Christensen S E, Koski O. 2-Dimensional waveguide coherent beam combiner. In: Proceedings of Advanced Solid-State Photonics. Washington: Optical Society of America, 2007. WC1
250 Uberna R, Bratcher A, Alley T G, et al. Coherent combination of high power fiber amplifiers in a two-dimensional re-imaging waveguide. Opt Express, 2010, 18: 13547–13553
251 Uberna R, Bratcher A, Tiemann B G. Coherent polarization beam combination. IEEE J Quantum Electron, 2010, 46: 1191–1196
252 Ma P F, Zhou P, Su R T, et al. Coherent polarization beam combining of eight fiber lasers using single-frequency dithering technique coherent polarization beam combining of eight fiber lasers. Laser Phys Lett, 2012, 9: 456–458
253 Kozlov V A, Hernández-Cordero J, Morse T F. All-fibercoherent beam combining of fiber lasers. Opt Lett, 1999, 24: 1814–1816
254 Montoya J, Hwang C, Martz D, et al. Photonic lantern kW-class fiber amplifier. Opt Express, 2017, 25: 27543–27550
255 Su R, Zhou P, Wang X, et al. Impact of temporal and spectral aberrations on coherent beam combination of nanosecond fiber lasers. Appl Opt, 2013, 52: 2187–2193
256 Yu H L, Ma P F, Wang X L, et al. Influence of temporal-spectral effects on ultrafast fiber coherent polarization beam combining system. Laser Phys Lett, 2015, 12: 105301
257 Klenke A, Seise E, Limpert J, et al. Basic considerations on coherent combining of ultrashort laser pulses. Opt Express, 2011, 19: 25379–25387
258 Su R, Zhou P, Wang X, et al. Active coherent beam combination of two high-power single-frequency nanosecond fiber amplifiers. Opt Lett, 2012, 37: 497–499
259 Su R, Zhou P, Ma Y, et al. 1.2 kW average power from coherently combined single-frequency nanosecond all-fiber amplifier array. Appl Phys Express, 2013, 6: 122702
260 Ma P, Tao R, Wang X, et al. Coherent polarization beam combination of four mode-locked fiber MOPAs in picosecond regime. Opt Express, 2014, 22: 4123–4130
261 Zhou P, Wang X, Ma Y, et al. Stable coherent beam combination by active phasing a mutual injection-locked fiber laser array. Opt Lett, 2010, 35: 950–952
262 Zhou P, Ma Y, Wang X, et al. Coherent beam combination of a hexagonal distributed high power fiber amplifier array. Appl Opt, 2009, 48: 6537–6540
263 Zhou P, Ma Y, Wang X, et al. Coherent beam combination of three two-tone fiber amplifiers using stochastic parallel gradient descent algorithm. Opt Lett, 2009, 34: 2939–2941
264 Su R, Zhou P, Wang X, et al. Actively coherent beam combining of two single-frequency 1083 nm nanosecond fiber amplifiers in low-repetition-rate. IEEE Photon Technol Lett, 2013, 25: 1485–1487
265 Chen Z, Zhou P, Wang X, et al. Synchronization and coherent addition of three pulsed fiber lasers by mutual injection and phase modulation. Opt Laser Tech, 2009, 41: 710–713
266 Zhou P, Wang X, Chen Z, et al. Coherent combining of two pulsed fibre lasers in phase modulated mutually coupled fibre laser array. Electron Lett, 2008, 44: 1238–1239
267 Ma P, Zhou P, Wang X, et al. Influence of perturbative phase noise on active coherent polarization beam combining system. Opt Express, 2013, 21: 29666–29678
268 Ma P, Wang X, Ma Y, et al. Analysis of multi-wavelength active coherent polarization beam combining system. Opt Express, 2014, 22: 16538–16551
269 Ma P, Lü Y, Zhou P, et al. Investigation of the influence of mode-mismatch errors on active coherent polarization beam combining system. Opt Express, 2014, 22: 27321–27338
270 Ma P F, Zhou P, Ma Y X, et al. Coherent polarization beam combining of four high-power fiber amplifiers using single-frequency dithering technique. IEEE Photon Technol Lett, 2012, 24: 1024–1026
271 Ma P, Zhou P, Xiao H, et al. Generation of a 481-W single frequency and linearly polarized beam by coherent polarization locking. IEEE Photon Technol Lett, 2013, 25: 1936–1938
272 Ma P, Zhou P, Wang X, et al. Coherent polarization beam combining of four 200-W-level fiber amplifiers. Appl Phys Express, 2014, 7: 022703
273 Liu Z, Zhou P, Ma P, et al. 5 kW level laser generation by coherent polarization beam combining of four high-power narrow-linewidth linearly-polarized fiber amplifiers (in Chinese). Chin J Laser, 2017, 44: 0415001–0415004
274 Bochove E J, Ray W, Durville F, et al. A linear model for passive coherent combining a large number of fiber lasers. In: Proceedings of Advances in Optical Materials. Washington: Optical Society of America, 2012. JTh2A-19

275 Shamir Y, Zuitlin R, Sintov Y, et al. 3kW-level incoherent and coherent mode combining via all-fiber fused Y-couplers. In: Proceedings of Frontiers in Optics. Washington: Optical Society of America, 2012. FW6C-1
276 Redmond S M, Ripin D J, Yu C X, et al. Diffractive coherent combining of a 25 kW fiber laser array into a 19 kW Gaussian beam. Opt Lett, 2012, 37: 2832–2834
277 Yu H L, Zhang Z X, Wang X L, et al. High average power coherent femtosecond pulse combining system based on an all fiber active control method. Laser Phys Lett, 2018, 15: 075101
278 Kienel M, Müller M, Klenke A, et al. 12 mJ kW-class ultrafast fiber laser system using multidimensional coherent pulse addition. Opt Lett, 2016, 41: 3343–3346
279 Müller M, Klenke A, Stark H, et al. High-energy 1.8 kW 16-channel ultrafast fiber laser system. In: Proceedings of SPIE, San Francisco, 2018. 1051208
280 Zervas M N. Power scalability in high power fibre amplifiers. In: Proceedings of Conference on Lasers and Electro-Optics Europe & European Quantum Electronics Conference (CLEO/Europe-EQEC), 2017
281 Steinke M, Tünnermann H, Kuhn V, et al. Single-frequency fiber amplifiers for next-generation gravitational wave detectors. IEEE J Sel Top Quant Electron, 2018, 24: 1–13
282 Johnson M C, Brunton S L, Kundtz N B, et al. Extremum-seeking control of the beam pattern of a reconfigurable holographic metamaterial antenna. J Opt Soc Am A, 2016, 33: 59–68
283 Fu X, Brunton S L, Nathan Kutz J. Classification of birefringence in mode-locked fiber lasers using machine learning and sparse representation. Opt Express, 2014, 22: 8585–8597